Exploring Novel Approaches to Combat Antibiotic Resistance via Cryptic Pockets: A Revised and Updated Review

Joshi Ankur[1], Soni Priyanka[2], Khemani Purva[1], Jain K. Neetesh[1], Shaikh Gulfisha[1], Manglawat Shailendra[1], Koshta Ashok[1], Malviya Sapna[1] and Kharia Anil[1]

ABSTRACT

The emergence of antibiotic-resistant diseases in both humans and animals poses a serious risk to public health around the world. In order to combat antibiotic resistance, new antibiotics are crucial. Cryptic binding sites could be useful in developing drugs to combat antibiotic resistance, as finding new targets is challenging. New targets are hard to come by; therefore, this is vital. How effective cryptic pockets are in combating antibiotic resistance is, unfortunately, unknown. The role of cryptic pockets in preventing antibiotic resistance is investigated in this study. The roots of and reasons for antibiotic resistance are initially investigated. After that, we move on to the topic of antibiotic resistance prevention and the potential advantages of cryptic pockets. Additionally, this case study demonstrates the utilization of a tailored inhibitor and the presence of cryptic pockets in resistance proteins. This review examines cryptic pockets and how they can be used to combat antibiotic resistance in future pharmaceutical development efforts.

Keywords: Antibiotic resistance, Cryptic pocket, New pocket, Reducing resistance

[1]Modern Institute of Pharmaceutical Sciences, Indore, Madhya Pradesh, India ROR
[2]Sri Aurovindo Institute of Pharmacy, Indore, Madhya Pradesh, India

Correspondence to: Joshi Ankur, ankurpharmacology@gmail.com

Cite this as: Ankur J, Priyanka S, Purva K, Neetesh JK, Gulfisha S, Shailendra M, Ashok K, Sapna M, Anil K. Exploring Novel Approaches to Combat Antibiotic Resistance via Cryptic Pockets: A Revised and Updated Review. Premier Journal of Infectious Diseases 2026;6:100006

DOI: https://doi.org/10.70389/PJID.100006

Peer Review:

Received: 10 October 2025

Last revised: 31 December 2025

Accepted: 11 May 2026

Version accepted: 2

Published: 18 May 2026

Ethical approval: N/a

Consent: N/a

Funding: N/a

Conflicts of interest: N/a

Author contribution: Joshi Ankur: Writing–review; editing

Guarantor: Joshi Ankur

Provenance and peer-review: Unsolicited and externally peer-reviewed

Data availability statement: N/a

Introduction

Antibiotic resistance is a public health issue that is worsening, and also results in the death of patients. The annual mortality due to antibiotic resistance is 700,000.[1] Antibiotic resistance might cost $300 billion to $1 trillion in global capital by 2050.[2] Bacterial infections induced by resistant microorganisms are a major public health issue because they prolong illness and increase mortality.[3] This is especially true for immunocompromised patients. Antibiotic resistance must be addressed to lower mortality.

Recent medication research has helped fight antibiotic resistance. Well-known β-lactam antibiotics have long been used to treat infectious infections.[4] As per Williams,[5] β-lactam antibiotics like cephalosporins, penicillins, carbapenems, and monobactams share similar structures. While C-7 substituents improve antibiotic potency and selectivity, β-lactamase diarylation reduces their efficacy.[6] Antibiotic resistance cannot be tackled by active pocket technology inhibitors for antibiotic-resistant bacterial proteins. Cryptic binding regions can allosterically affect protein activity despite being far from the catalytic domain.[7,8] A new drug may target them. To overcome antibiotic resistance, there is a need to create and test structurally distinct medicines that attack cryptic areas.

New cryptic pocket inhibitors restore antibiotic susceptibility. Cryptic pockets have been utilized to explore antibiotic resistance produced by gene mutations in HPPK, LpXH, FP-2, DHPS, FtsZ, MDH, β-lactamase, and DsbA.[9–15] Dennis et al. found 8MG HPPK cryptic pocket compounds. Dennis et al.[16] found that substances with Kd values of 0.21–0.965 μM inhibited the enzymes SaHPPK and EcHPPK. A strain of E. coli overexpressing LpXH was used for high-throughput screening. To test drugs, MIC measurements were taken at doses ranging from 3 to 200 μM.[17] AZ1 (1) inhibits E. coli mutants with a 0.25 μg/mL MIC value by adhering to an L-shaped cryptic pocket with indoline and piperazine moieties, far from the active site. Identification of cryptic gaps can help fight antibiotic-resistant bacteria and viruses. Cryptic pockets and antibiotic resistance have scarcely been studied.

We will describe how well encrypted pockets fight antibiotic resistance. We begin with a description of the history of antibiotic resistance, its targets, inhibitors, and mechanisms from 1960 to 2023. Section two addresses antibiotic resistance using cryptic pockets. We discuss binding conformation, protein activity, resistance, and new inhibitors that interact with cryptic pockets to target resistant targets. This review can help biologists and chemists uncover antibiotic-resistant compounds and cryptic niches.

Antibiotic Resistance

The Incidence of Antibiotic Resistance

Antibiotic resistance research aids epidemic response and drug selection.[18,19] Nosocomial infections are caused by treatment-resistant ESKAPE bacteria like *Pseudomonas aeruginosa*, *Staphylococcus aureus*, *Klebsiella pneumoniae*, *Acinetobacter baumannii*, and *Staphylococcus* spp.[20] Due to their structure, most ESKAPE bacteria are drug-resistant.[21] *Carbacechella pneumoniae* (CRKP) may be drug-resistant due to plasmid exchange and pathogenicity.[22] The WHO identified Acinetobacter baumannii as one of 12 "key pathogens" in 2017 that required quick administration of antimicrobial medications.[23] Bacillus catalase peroxidase had the most mutations of the 33 targets that we studied. There were 20 antibiotic resistance targets for isoniazid and seven for cephalosporins.[24] Figure 1A shows that antibiotic resistance has been decreasing since the 1990s. Antibiotic use is increasing, and while resistance declined slightly in the 1990s, a comprehensive plan is needed to reverse this trend.

Mechanisms of Antibiotic Resistance

Prevention of antibiotic resistance requires an understanding of its mechanisms.[25] Non-target actions such antibiotic modification/biodegradation, membrane permeability decrease, efflux pump overexpression or expression, target modification/competitive binding, bypassing, or protection might cause antibiotic resistance (Figure 1B).[26] We will discuss the prevalence and impact of each resistance mechanism on bacterial biology.

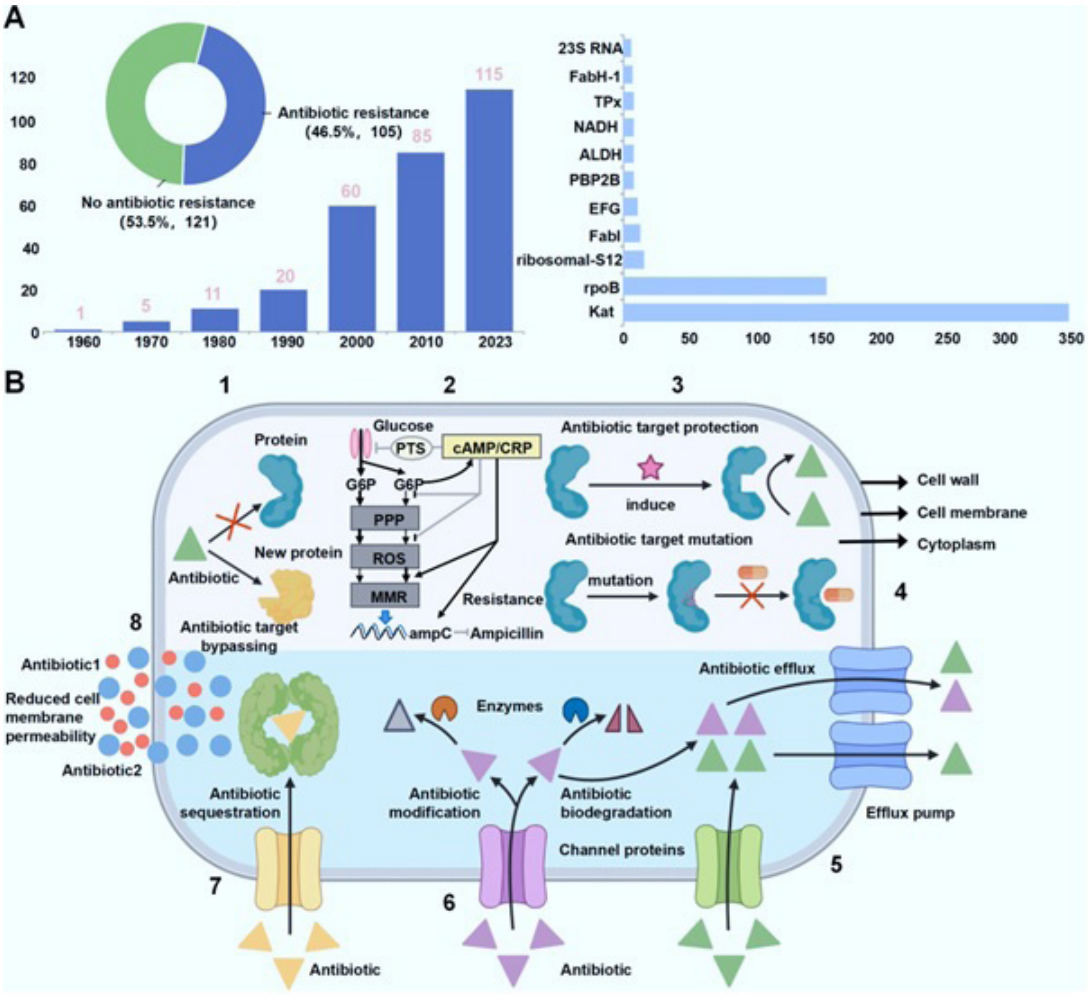

Fig 1 | Antibiotic resistance is widespread. Antibiotic resistance is increasing. Out of 227 targets, 106 were antibiotic-resistant. The image illustrates antibiotic-resistant target numbers and mutation sites from 1966 to 2022. FabH: 3-oXoacyl-[acyl-carrier-protein] reductase; 1. (B) Antibiotic resistance. Examples include modification/biodegradation, protein sequestration, mutation, protection, competitive binding,[32] antibiotic target bypass, and reduced cell membrane permeability

Target resistance has four main causes. Antibiotic target bypassing creates a metabolic route that avoids the antibiotic's native target, eliminating its effects. When traditional medicines fail, the cell's DNA may mutate to generate desired traits.[27] An increase of methicillin S. aureus-intolerant bacteria led to avoidance of targeting. S. aureus acquired penicillin-binding protein 2a and became methicillin-resistant. While similar to targeted PBPs, this protein exhibits a lower affinity for β-lactam drugs.[28,29] Another example is vancomycin-resistant enterococcal strains. Vancomycin, unlike β-lactam antibiotics, inhibits cell wall production by binding to pentapeptide precursors' final D-alanine residues, serving as a substrate for PBPs. Enterococcus bacteria usually gain vancomycin resistance from a cluster of van genes in transposon Tn1546. The genetic modification converts D-alanine-D-alanine into D-lactate or D-serine. Both the new structures have lower vancomycin affinity.[30,31] Bacteria become antibiotic-resistant when their metabolites compete with antibiotic-binding proteins. Ampicillin blocks PDH and the pts promoter to reduce glycolysis and boost glucose transfer. The pentose phosphate pathway produces glucose-derived ROS to modify genes. Ampicillin restores PDH function and lowers blood sugar by blocking pyruvate competitive inhibition and activating the aAMP/cAMP receptor protein complex.

This signaling cascade reduces glucose transport and ROS for DNA repair and ampicillin resistance. Pathogens' ampicillin resistance depends on glucose.[32] Mutations from antibiotic pressure are a third target-based resistance mechanism. Multiple gene modifications can result from a single-nucleotide mutation. These structural changes prevent antibiotics from binding to the protein, and yet, it still works.[33] When patients have an infectious disease, their pathogen susceptibility changes. One nucleotide change makes an antibacterial target gene antibiotic-resistant, allowing the organism to multiply faster.[33] Linezolid, the first oxazolidinone antibiotic, targets the 23s rRNA ribosomal subunit, since every gene has two copies.

DOI: https://doi.org/10.70389/PJID.100006 | Premier Journal of Infectious Diseases 2026;6:100006

Gram-positive bacteria can gain linezolid resistance by mutating homologous alleles and forming a mutant population.[34,35]

Mutations in some regions or "mosaic" gene types may cause antibiotic resistance after acquiring genomic material from outside sources. *Streptococcus pneumoniae* is the classic mosaic penicillin-binding protein (pbp)-resistant bacteria. These mosaic genotypes received their genomes from *Streptococcus mitis*, a phylogenetically distinct species. Mosaicism in the PBP-enclosing pena gene confers Neisseria gonorrhoeae with strong extended spectrum cephalosporin resistance.[36,37] As a fourth target-based resistance approach, antibiotic target protection alters the primary target's structure or protects it by modifying amino acids, phosphorylation, glycosylation, methylation, or acetylation.[33] As the target protein structure changes, the antibiotic–protein interaction weakens, causing resistance.[38]

Target modification-induced resistance affects amidoglycosides, daptomycin, streptogramins, pleuromutilins, macrolides, oxazolidonones, lincosamines, polymyxins, phenicols, and quinolones.[39] The erythromycin ribosome methylase (erm) genetic lineage methylates 16S rRNA, altering drug-binding sites and decreasing streptogramin, lincosamine, and macrolide affinity.[40] A2503 is selectively methylated by the cfr methyltransferase to make 23S rRNA resistant to phenicols, oxazolidinones, streptogramins, pleuromutilins, and lincosamines.[41] Target modification resistance is complex. Non-target activity includes efflux pump overexpression, antibiotic modification or biodegradation, sequestration, and membrane permeability reduction. Energy-dependent antibiotic export by transmembrane efflux pumps is the main cause of gram-negative bacteria resistance.[42] Substrate-specific efflux pumps and multidrug resistance (MDR) transporters can transport many drugs with various architectures and activities.[43] Previous investigations have shown that DrrAB transfers doxorubicin and daunorubicin from Streptomyces peucetius via ATP or GTP to acquire the MDR phenotype.[44,45] RND pumps are MDR pumps because they export several antibiotics. By overexpressing this gene, N. gonorrhoeae can become resistant to penicillin, azithromycin, tetracycline, third-generation cephalosporins, and mtrCDE, its RND pump.[46–48] Biodegradation and modification reduce antibiotic action significantly.[49] Different enzymes can break down and alter antibiotics such as macrolides, phenicols, and aminoglycosides. *Acinetobacter baumannii*, *Pseudomonas aeruginosa*, *Escherichia coli*, and *Klebsiella pneumoniae* develop resistance to β-Lactam antibiotics because β-lactamases break down clavams, monobactams, penicillins, carbapenems, and cephalosporins.[50–53] Flavin-dependent monoxygenase Tet X hydroxylates alkyl groups at position 11a in tetraketides. Antibiotics that cannot attach to the 30S ribosome due to structural changes generate high antibiotic resistance.[54]

Antibiotic sequestration involves proteins binding to drugs and blocking their targets.[55] Overexpressed TlmA, ZbmA, and BlmA proteins make streptoalloteichus, streptomyces verticillus, and streptomyces flavoviridis resistant to bleomycin. These proteins isolate metal-bound or metal-free antibiotics.[56–59] Streptomyces spp.'s β barrel-like TnmS1, TnmS2, and TnmS3 structures sequester tiancimycins with nanomolar affinity, resulting in CB03234 resistance.[60] Less permeable membranes reduce bacteria antibiotic accumulation. Low glutamine affects nucleoside synthesis and inosine levels. This lowers intracellular antibiotic accumulation and bacterial non-specific membrane permeability by altering CpXA/ApXR and OmpF expression. Antibiotic resistance can occur when bacteria become less sensitive to lower antibiotic concentrations.[61] Bacterial export or alteration of antibiotics is a proven, non-specific antibiotic resistance mechanism.

Cryptic Hiding Places to Decrease Antibiotic Resistance

Details About Cryptic Pockets

When fragmented protein molecules bind with targets, crypto pockets emerge (Figure 2A).[62,63] These novel binding sites may help pharmaceutical designers find "undruggable" proteins and eliminate drug resistance. Multiple studies show that ligand interaction changes protein-binding pockets.[63] Treatment of resistance phenotypes requires an understanding of cryptic pockets. Cryptic pockets are less likely to contain ligands,[64] are more hydrophobic and flexible,[8] can modulate protein biological activity even when far from functional regions,[65] and can change the active site structure, increasing drug affinity.[64] Cryptic pockets have been in the headlines recently, but their unique properties make them difficult to diagnose and treat.

Approaches to Reduce Antibiotic Resistance Through the Use of Cryptic Pockets

We propose eight ways to reduce protein antibiotic resistance using cryptic pockets: bypassing, enzymatic modification, dual targeting, lowering antibiotic sequestration, efflux, and identifying novel pockets. Each technique reduces antibiotic resistance as shown above.

New pockets, dual targeting, prevention, signal transduction interference, and bypassing can overcome antibiotic resistance. By targeting underexploited cryptic areas, rational drug design can degrade target protein biological activity and combat drug resistance (Figure 3A). Inhibitors change the active site shape by binding to cryptic pockets in drug targets, restoring drug-active site-binding affinity. Dual aiming is shown in Figure 3B. Drugs that target drug-resistant target proteins in their active and cryptic domains may be more successful. Targeting cryptic and active areas prevents or delays drug resistance (Figure 3C). Cryptic pockets in proteins in a similar signaling cascade (upstream and downstream) as resistance proteins can affect pathogen infection and compensate for resistance target sensitivity loss by interfering with signal transduction (Figure 3D).

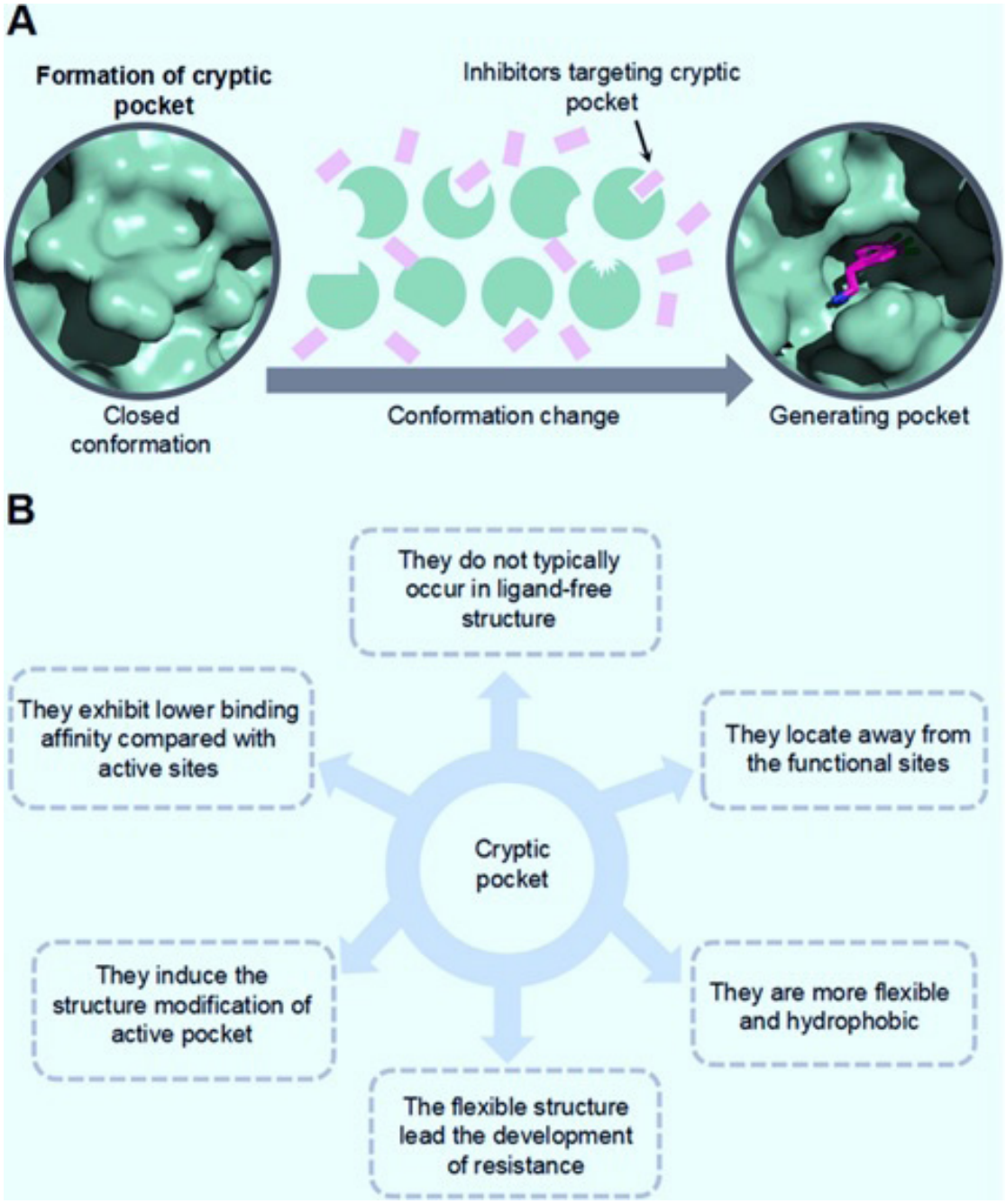

Fig 2 | Properties of cryptic pockets. Cryptic pockets as new drug-binding sites. (B) Their location, flexibility, resistance development, structural alteration, and binding affinity advantages over active pockets

According to the bypass, other pathogenic and drug-resistant proteins may use cryptic pockets. Figure 3E reveals that hidden binding site inhibitors reduce resistant pathogen pathogenicity, but do not stop development. Cryptic pockets affect enzyme modification, efflux, and sequestration, restoring treatment efficacy and reducing non-target process resistance. Inhibitors that target efflux pump cryptic pockets lower efflux channel size and efficacy (Figure 3F). A decrease in bacterial drug efflux increases cell drug concentration, affecting protein function and disease risk. In Figure 3G, inhibitors of antibiotic-modifying enzymes (e.g., β-lactamases, acetyltransferases, phosphotransferases, and nucleotidyl transferases) target their cryptic pockets to reduce or stop antibiotic modification and deactivation. Figure 3H shows how proteins can block medication routes. Sequestering protein cryptic region inhibitors can modify antibiotic sequestration and drug binding to target proteins. Identifying novel pockets, interfering with signal transduction, prevention, bypass, or enzyme modification are seven ways in which crypto pocket inhibitors reduce antibiotic resistance (Table 1).

DOI: https://doi.org/10.70389/PJID.100006 | Premier Journal of Infectious Diseases 2026;6:100006

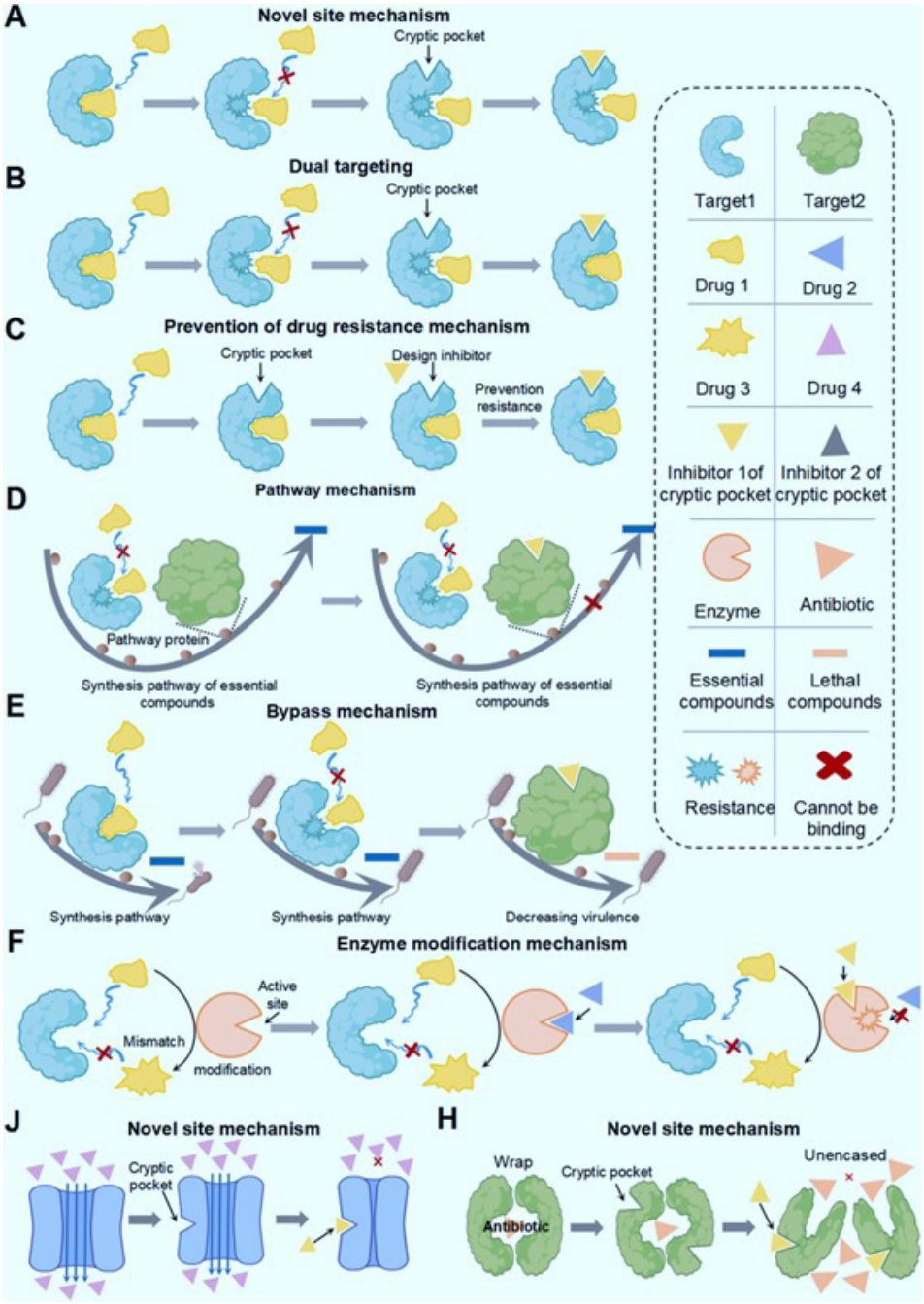

Fig 3 | Antibiotic resistance reduction through cryptic pocket access. Cryptic pocket antibiotics diminish resistance by altering protein function. (B) Antibiotic binding in the cryptic pocket changes the active site conformation, increasing drug-binding affinity with both pockets. Cryptic environments slow antibiotic resistance. A cryptic pocket targeting protein in the same signaling pathway as resistance targets can disrupt signal transmission. Cryptic pockets diminish antibiotic resistance by reducing pathogenic virulence while maintaining pathogenicity. Antibiotic-modifying enzymes develop resistance, and inhibitors targeting cryptic pockets can limit their inactivation of antibiotics. Cryptic pockets also decrease antibiotic efflux and control the protein structure that influences antibiotic sequestration

The Development of Inhibitors Targeting Cryptic Pockets in Antibiotic Targets

Targeting Novel Pockets

6-Hydroxymethyl-7,8-Dihydropterin Pyrophosphokinase (HPPK)

HPPK must transfer a pyrophosphate moiety from ATP to 6-hydroxymethyl-7,8-dihydropterin (DHP) to create folate cofactors.[66] Folate synthesis begins with HP. HP is needed for several carbon-atom transfer processes.[67] Folic acid synthesizes amino acids, purines, and pyrimidines for cell metabolism, growth, and function.[68] Prokaryotic and lower eukaryotic microbes manufacture folate using HPPK, but mammals and other higher eukaryotic organisms source it from their diet.[66] DHPPP is formed when the tiny 18 Kda protein HPPK aids the magnesium-dependent conversion of pyrophosphate

Table 1 | Inhibitors targeting cryptic pockets to reduce antibiotic resistance

Name	Unbound	Bound	Ligands	Affinity	Resistance Mechanism	Mechanism for Reducing Resistance
6-hydroxymethyl,7,8-dihydropterin pyrophosphokinase (HPPK)	1Q0N	4M5G	Compound 1 (1)	IC_{50} = 139 μM	Target mutation	Novel pocket discovery: Crypticbinding sites are different and distant from the active pockets in resistance targets that can provide novel pockets for drug design, producing drugs that disrupt the biological function of target proteins
		4M5H	Compound 2 (2)	IC_{50} = 254 μM		
		-	Compound 3 (3)	IC_{50} = 64 μM		
		-	Compound 4 (4)	IC_{50} = 82 μM		
		-	Compound 5 (5)	IC_{50} = 79 μM		
		-	Compound 6 (6)	IC_{50} = 88 μM		
		-	Compound 7 (7)	IC_{50} = 51 μM		
		-	Compound 8 (8)	IC_{50} = 51 μM		
		-	34 (9)	Kd = 0.33 μM		
		-	40 (10)	Kd = 0.30 μM		
		-	47 (11)	Kd = 0.965 μM		
		-	48 (12)	Kd = 1.4 μM		
		-	49 (13	Kd = 0.95 μM		
Dihydropteroate synthase (DHPS)	3TYE	4NHV	2O6	-	Target mutation	Novel pocket discovery
		4NIL	2O8	-		
		4NIR	6DH			
		4NL1	Z13	Kmobs = 99 μM		
		-	Compound 1 (14)			
		-	Compound 2 (15)			
		-	Compound 3 (16)			
		-	Compound 4 (17)			
		-	Compound 5 (18)			
		-	Compound 6 (19)			
		-	Compound 7 (20)			
		-	Compound 8 (21)			
		-	Compound 9 (22)			
		-	Compound 10 (23)			
		-	Compound 11 (24)	IC_{50} = 17–50 μM		
UDP-diacylglucosamine pyrophosphohydrolase (LpxH)	6PH9	6PIB	AZ1 (25)	IC_{50} = 0.36 μM	Target mutation	Novel pocket discovery
		6PJ3	JH-LPH – 33 (26)	IC_{50} = 0.026 μM		
		6PII	JH-LPH – 41 (27)	-		
		-	JH-LPH – 28 (28)	IC_{50} = 0.011 μM		
Filamentous thermosensitive protein Z (FtsZ)	2Q1X	6Y1U	Coumarin (29)		Target mutation	Novel pocket discovery
			4HC (30)	IC_{50} = 200 μM		
Malate dehydrogenase (MDH)	6R8G	6Y91	4DT (31)	Kd = 99 μM	Target mutation	Novel pocket discovery
		-	Compound 1b (32)	40% reduction		
		-	Compound 2b (33)	35% reduction		
		-	Compound 4a (34)	35% reduction		
		-	Compound 4b (35)	80% reduction		
		-	Compound 5a (36)	48% reduction		
		-	Compound 5b (37)	47% reduction		

DOI: https://doi.org/10.70389/PJID.100006 | Premier Journal of Infectious Diseases 2026;6:100006

Table 1 | Continued

Name	Unbound	Bound	Ligands	Affinity	Resistance Mechanism	Mechanism for Reducing Resistance
		-	Compound 7a (38)	77% reduction		
		-	Compound 9a (39)	49% reduction		
		-	4PA (40)	Ki = 12.5 mM		
TEM-1 β-lactamase	1BTL	1PZO	Compound 1 (41)	Ki = 490 μM	Antibiotic modification/ biodegradation	Enzyme modification: Inhibitors targeting cryptic pockets in enzymes that modify the structure of antibiotics can decrease or inhibit the modification and inactivation of antibiotics
		1PZP	Compound 2 (42)	Ki = 480 μM		
		-	NSC350086 (43)	EC_{50} = 162 μM		
		-	NSC333009 (44)	EC_{50} = 63 μM		
		-	NSC341597 (45)	EC_{50} = 57 μM		
		-	ZINC12026660 (46)	-		
		-	ZINC19908919 (47)	-		
		-	ZINC40961289 (48)	-		
		-	ZINC11957607 (49)	-		
		-	ZINC23109855 (50)	-		
Disulfide-bond formation protein A (DsbA)	3KDS	7LUH	NHX (51)	-	Target bypass mechanism	Bypass pathway: Inhibitors targeting cryptic pockets in another protein can decrease antibiotic resistance in humans by decreasing the virulence of pathogens, while leaving the pathogenic bacterial growth pathways intact
		YCS (52)		-		

from ATP into DHP.[69] Two necessary Mg2+ ions coordinate the triphosphate moiety of ATP, and a conserved gap between enzyme loop portions holds the adenosine ring in place. DHP places the pterin ring between two well-preserved aromatic amino acid residues in a nearby molecular pocket.[70] A detailed investigation of ligand-free HPPK compared to its tripartite complex with DHP and ATP found that loops 1–3 are HPPK's functional location.[71] Catalytic residues R82 and R92 now occupy the optimum Mg-ATP-binding site due to the conformational shift.[72,73] HPPK-targeted drugs are important because DHPS mutations reduce the efficacy of sulfa-containing antibiotics.[74] The lack of an HPPK substrate and catalytic process expertise complicates active site drug design.[75]

Virtual screening and X-ray crystallography revealed a W89-L45 cryptic pocket near HPPK's pterin-binding site. Computer simulations of HPPK–pharmacological candidate interactions showed conformational changes.[76] Virtual screening predicts that the protein will interact with several small ligands, revealing a cryptic pocket through conformational changes. X-ray crystallography validated and captured high-resolution static HPPK structures down to the atomic level, revealing the cryptic pocket structure. Many HPPK inhibitors were found via high-throughput screening in 2014. One of these compounds modified loops 2 and 3 with an aryl-substituted 8-thiaoguanine scaffold, displacing L45, W89, and R92. Thus, an extra pocket was generated next to the pterin-binding pocket (Table 1; Figure 4A, B).[74] X-ray crystallography showed that 1 and 2 interact with HPPK's active site and cryptic pockets. The pterin pocket squeezed free 8-thioguanine between Y53 and F123, which created precise hydrogen bonds with residues T42 and N55's side chain moieties due to its nitrogen and oxygen atoms. The nucleotide's α- and β-phosphate moieties are coupled to R82 and R92 in the cryptic pocket via salt bridges created with D95 via the 8-thio substituent. 1 and 2 bonded to an HPPK, AMPCPP, and DHP ternary complex. The carbonyl group in the linker between 8-thioguanine and phenyl rings may be responsible for the higher HPPK inhibition in structure 1 (Kd = 9.7 μM and IC_{50} = 139 μM) compared to structure 2 (Kd = 29 μM and IC50 = 254 μM).[74] The phenyl ring replacements 3–8 resulted in increased inhibitory effectiveness (IC_{50} = 44–88 μM), likely due to the carbonyl moiety in 1. Smaller replacements on 1, such as 3, 4, 5, 7, and 8, were favored over larger ones, such as 6. The optimized ternary complexes showed that phenyl groups 3 and 7 could access the protein's cryptic pocket within 1 Å, unlike group 1 (Figure 4C). These stacking interactions strengthened the connection between R121's guanidine groups and 1's flat carbonyl. SARs set a standard for structural change based on these molecules' pharmacological and biophysical

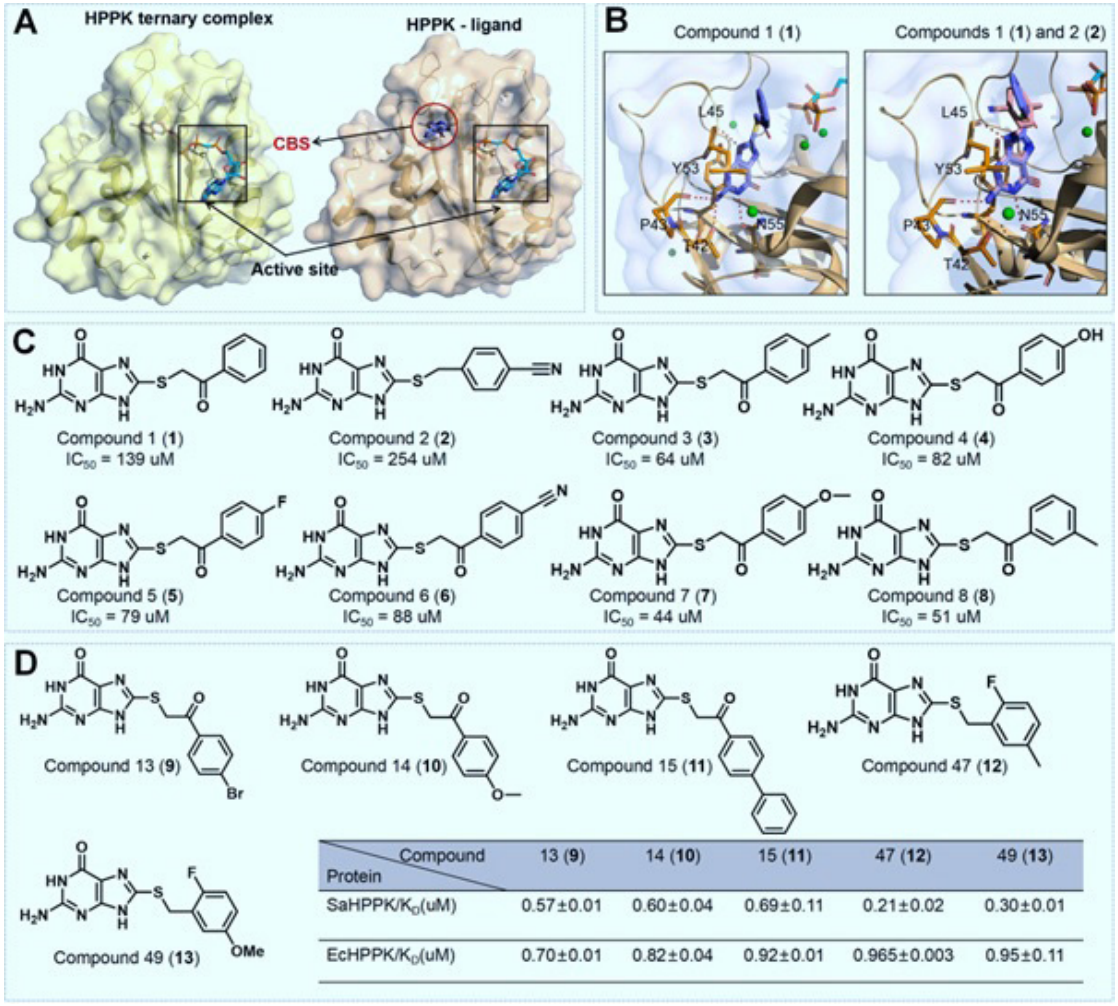

Protein \ Compound	13 (9)	14 (10)	15 (11)	47 (12)	49 (13)
SaHPPK/K_D(uM)	0.57±0.01	0.60±0.04	0.69±0.11	0.21±0.02	0.30±0.01
EcHPPK/K_D(uM)	0.70±0.01	0.82±0.04	0.92±0.01	0.965±0.003	0.95±0.11

Fig 4 | Cryptic pocket-based HPPK inhibitors. Pre- and post-exposure E. coli HPPK cryptic pocket (PDB ID-unbound: 1Q0N; bound: 4M5G Compounds 1 and 2 bind HPPK's cryptic pocket (4M5G, 4M5H). Potent and representative HPPK 8-thioguanine scaffold derivative inhibitors. D) Small-molecule cryptic pocket halogenated 8-thioguanine scaffold derivative inhibitors

properties.[74] Using the model (Figure 4D),[16] we determined the binding conformations of 8MG and its S-benzylated derivatives, which had electronegative and electropositive moieties in the aromatic rings at ortho, meta, and para positions in the cryptic pocket. X-ray crystallographic studies show that the cryptic pocket binding behavior is identical to that of S-benzylated 8MG derivatives, including those with a p-cyanobenzyl-substituent (1.96 Å). The structure connects the guanine moiety of 10 to the protein via six hydrogen bonds. The core heterocyclic motif stacks π-electronically with the aromatic components of F54 and F123. The benzyl group was found in the small gap produced by the thiol extension between loops 2 and 3 residues 47–51 and 84–91. The sulfur atom in 10 is now about 1 Å further away from the pocket, allowing the binding site to be optimally occupied. The aliphatic moieties amino acid residues P45, Y48, Q51, F54, and W89 exhibited hydrophobic interactions with the benzyl ring, while residues N11, Q51, G90, and P91 were electrostatically bound to the nitrile moiety. The inhibitory effect against EcHPPK was intensified by substituents, showing that compounds with m-methyl (11, Kd = 0.965 μM), p-fluoro (12, Kd = 1.4 μM), and p-methoxy (13, Kd = 0.95 μM) substituents had significantly higher binding affinity. The p-cyano (10) and p-fluoro (9) derivatives showed improved binding affinities to SaHPPK, with Kd values of 0.30 μM and 0.33 μM, respectively. Thus, lead compounds modified with halogen substituents showed greater promise as broad-spectrum HPPK inhibitors. The flexibility of the functional domain loop and critical residues makes the creation of highly potent HPPK inhibitors difficult. The cryptic binding sites around the main active sites may solve this problem. Since the SARs for both active site inhibitors and those binding in the cryptic pocket of HPPK have been established, this information can be utilized to change inhibitor structures and construct very effective antibiotics for this region. Further investigation is also required to determine how to crystallize the protein using the particular framework found in the cryptic pocket. An essential component

DOI: https://doi.org/10.70389/PJID.100006 | Premier Journal of Infectious Diseases 2026;6:100006

in optimizing potential inhibitors, such atomic resolution would yield an incontestable binding model between inhibitors and cryptic pockets.

Dihydropteroate Synthase (DHPS)

Bacteria metabolize p-aminobenzoic acid (pABA) and 6-hydroxy methyl-7,8-dihydropterin pyrophosphate (DHPPP) to dihydropteroate, an essential folic acid intermediary.[77,78] Dihydropteroate is generated when PABA's amino group displaces PPi from DHPPP.[79] Dihydropteroate produces nucleic acids during cell growth.[77] The complex's Fourier electron density map[80] reveals a conserved DHPPP-binding site in DHPS's eight-stranded α/β barrel structure, resembling a bent cylinder. DHPPP and pABA bind sequentially.[81] The C-terminal end of the β-strands has a deep gap, where DHPPP removes eight water molecules from the unliganded protein. In reference,[82] the dihydropterin moiety replaces others, while the γ-phosphate of DHPPP replaces one water molecule. Early DHPS antibiotics were sulfonamides.[83] Sulfonamide resistance increases 24 times in bacteria with DHPS gene mutations S382C, A383G, and A437G.[84] DHPS's amino acid sequence has changed over the past 70 years, making sulfathiazole and sulfadiazine ineffective.[85] A study detected sulfa-resistant *Plasmodium falciparum* in 96% of subjects.[86] DHPS's retained pterin-binding pocket has been exploited to develop new drugs.[87] This pocket favors pterin substrates and analogues, producing low-solubility pterin-like compounds.[88]

To produce sulfa-resistant drugs, new DHPS regions must be found. NMR and crystallographic investigations indicated a cryptic pocket at the DHPS interface for residues E260, L235, E236, and M264 (Figure 5A). Table 1 shows that DHPS inhibitors targeting cryptic pockets have pterin-like structures. Anthracis DHPS segments were screened with WaterLOGSY NMR and the 1100 chemical Maybridge Ro3 library. Ten of these compounds (14–23) target only the cryptic pocket.[87] Compounds 14–23 considerably reduced DHPS from Bacillus anthracis (86%), Yersinia pestis (61%), and *Staphylococcus aureus* (46%), while compounds 15–23 had very mild inhibitory effects at 250 μM. Imine 24, made from 14, completely inhibited DHP enzymes in three bacteria at 250 μM (Figure 5B). The IC_{50} values for this chemical were 50, 17, and 31 μM. Loop 7's X-ray cocrystal structure showed 24 additional residues linked to V231, E232, E233, R234, and L235. More interaction between loops 1 and 7 increases the possibility of loop 1 remaining in the active site and not releasing the product. Due to its weak physicochemical properties, it has little antibacterial activity, but it can be exploited as a lead molecule to develop stronger antimicrobials. Additional antifolate medicines and stronger cryptic pocket treatments could decrease resistance. X-ray co-crystal structural data of 11 derivatives can be used to increase drug-binding affinity to the cryptic pocket or inhibit DHPS's catalytic activity by interacting with pterin, PABA, and cryptic binding sites to reduce antibiotic resistance.

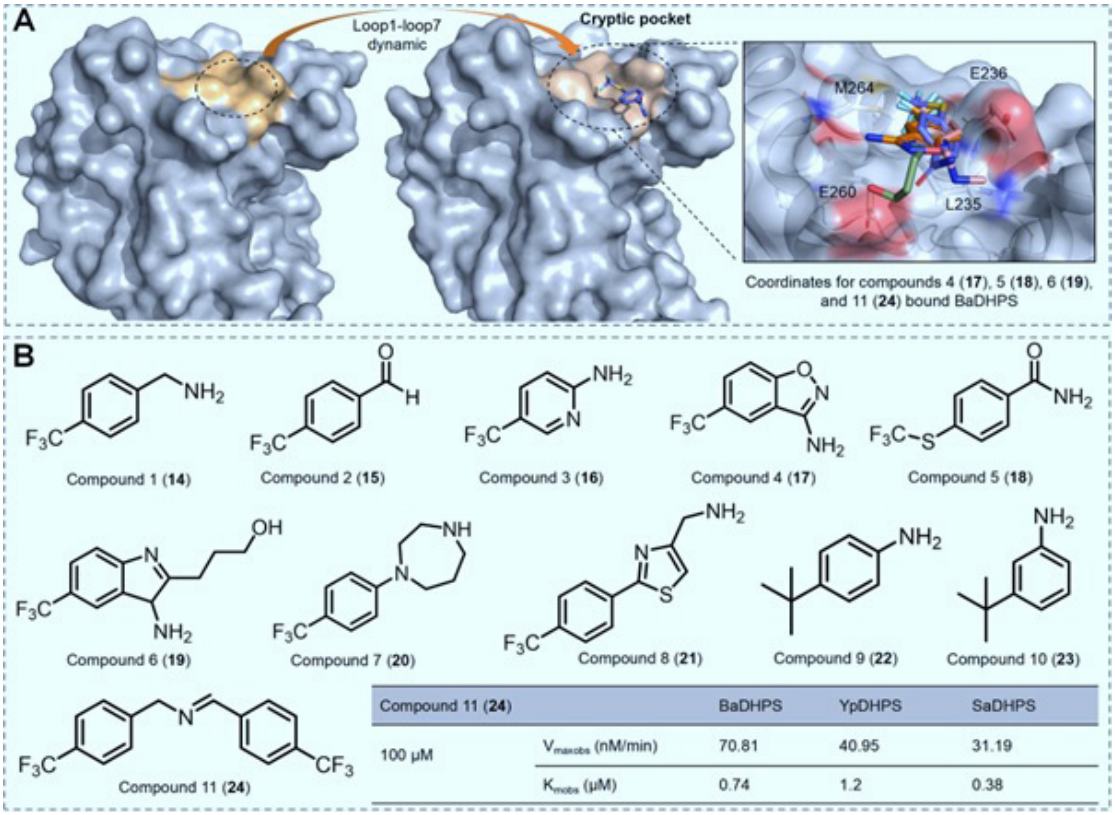

Compound 11 (24)		BaDHPS	YpDHPS	SaDHPS
100 μM	$V_{max obs}$ (nM/min)	70.81	40.95	31.19
	$K_{m obs}$ (μM)	0.74	1.2	0.38

Fig 5 | Discovery of DHPS cryptic pocket inhibitors. DHPS-assembled cryptic pocket and interaction structure of compounds 4 (17), 5 (18), 6 (19), and 11 (24). Structure of a cryptocurrency-targeting chemical

UDP-Diacylglucosamine Pyrophosphohydrolase (LpxH)

Stage 4 lipid The enzyme LpxH removes the pyrophosphate linkage from UDP-2,3-diacylglucosamine (UDP-DAGn) to produce lipid X.[89,90] This step initiates membrane-bound lipid A production. Gram-negative bacteria survive on lipid A, a hydrophobic lipopolysaccharide.[91] LpxH is a prospective therapy target because 70% of gram-negative bacteria use it as an enzyme.[92–94] Research indicates that LpxH contains just two central β-sheets, unlike PP-1, which has three in its core catalytic domain.[90] According to,[90] LpxH's two β-sheets form a separate structure that connects to β-sheet 2, forming two parallel β-chains. The "pitfall trap" cover plate in lipid X resembles the α2′ junction between α1′/α3′ helices.[95] Mn2+ ions' high electron densities in LpxH's functional motif, the core domain and insertion lid, affect enzyme performance.[96] D42 bridges the manganese clusters, binding Mn1, while D9, D11, N80, H195, and H196 bind Mn2.[97] By replacing these residues with alanine, LpxH's enzymatic activity decreases by 5,000 to 200,000.[90] No LpxH-active site conformation-specific drugs have been designed or tested.[98] Mutagenic experiments showed LpxH mutations G48D, L84R, F141L, and R149H to be protective against sulfonyl piperazine scaffold chemicals.[99] Gram-negative bacteria can avoid multidrug resistance with LpxH inhibitors. Locating LpxH's cryptic pockets may allow drug-resistant structural molecules.

Nuclear magnetic resonance (NMR) analysis of LpxH found an L-shaped hydrophobic chamber as a cryptic binding site and explained how it changed conformational and structural states (Figure 6A; Table 1). In a 384-well configuration, 1.2 million compounds were screened for enzyme activity at 50 μM doses.[99] AZ1 (25), a chemical compound with indoline and piperazine groups, inhibited E. coli efflux mutants at 0.25 μg/mL but not wild-type E. coli at concentrations above 64 μg/mL. Since 25 inhibited G48D, L84R, F141L, and R149H mutants 512-fold less than LpxH, it appeared to interact closely with them. 25 alters Gram-negative cell outer membrane biogenesis, making them antibiotic-resistant. 25 is hydrophobic and strongly binds protein in human plasma; hence, mammals should not get it.[99] Analogues of phenol, benzoic acid, and phenyl improved 25's physical characteristics. All derivatives (JH-LPH-4 to JH-LPH-26) demonstrated a 4- to 28-fold decrease in inhibitory efficacy compared to 25 (IC_{50} values: 0.14 μM for E. coli and 0.36 μM for Klebsiella pneumoniae). SARs showed a one AZ1 pharmacophore with one hydrogen-bond acceptor (carbonyl oxygen of the N-acetyl group on the indoline ring), two hydrophobic groups (indoline and piperazine rings), and two aromatic rings (benzene rings) for sulfonyl piperazine-based LpxH inhibitors.[100] 25 interacted with LpxH's L-shaped cavity, placing its indoline ring near the catalytic site (Figure 6B).[92] In K. pneumoniae LpxH, the indoline group formed complexes with lipophilic amino acids F82, L83, Y125, F128, I137, F141, I152, A153, and M156 by van der Waals contacts and cation–π stacking with R80. The acetyl group of 25 and LpxH residue N79 produced hydrogen connections, as did the sulfonamide moiety with residues R157 and W46. The LpxH-bound conformation of 25 was used to create two derivatives of 25: JH-LPH-33 (26) and JH-LPH-28 (28). These compounds were changed by adding chloro or fluoro derivative residues to the met a-configuration of the trifluoromethyl phenyl moiety. Chloro-substituted 26 showed stronger antibacterial activity, with IC_{50} values of 0.026 μM for K. pneumoniae and 0.046 μM for E. coil (Figure 6C). By contrast, fluoro-substituted 28 yielded IC_{50} values of 0.11 μM for K. pneumoniae and 0.083 μM for E. coli. With a halogenated group in the hydrophobic cavity, 26's inhibitory activity is 1.7 times stronger and 28's inhibitory activity is 13.8 times stronger. In JH-LPH-41 (27), a long acyl chain derivative of 26, poorer antibiotic action against K. pneumoniae LpxH (MIC = 32 μg/mL) was due to poor membrane penetration (Figure 6D).[95] SAR study showed a positive connection between chemical potency and functional moieties at the meta-position of the CF3-substituted distal aromatic ring. This site was most effective when H, F, CH3, and Cl were replaced in order to increase potency. New LpxH inhibitors could enable MDR research. Three factors prevent LpxH from using a cryptic pocket to reduce resistance: (1) the lack of a completely defined antibacterial activity profile for these inhibitors; (2) the need to modify their structural alterations to increase LpxH-binding affinity; and (3) the necessity to examine their effectiveness and selectivity for multidrug-resistant bacteria.

FtsZ Filamentous Thermosensitive Protein

Essential for bacterial cell division, a filamentous GTPase known as FtsZ forms a dynamic Z-ring within the cell.[101] Bacterial viability and dynamics are impacted when FtsZ assembly is disrupted.[102] The key cell division protein in the majority of bacteria is FtsZ, which creates a dynamic Z ring close to the split site. During cell division, GTP regulates the reassembly of the cell wall and the contraction of the filaments.[103] Inherent polymerization properties of FtsZ, including GTPase activity and lateral connections, govern its dynamics. These factors impact cellular elongation, division, and the recruitment and distribution of cell wall synthases.[104] A central helix (H7) is located in the N-terminal domain of FtsZ, which is connected to a C-terminal nucleotide-binding domain; protofilaments are formed by the C-terminal domain.[105,106] The GTPase-active site is located between the monomers that make up the FtsZ subunits.[105] A particular T7 ring and the GTP-binding site combine to create the active site.[106] G196S and G193D are the most prevalent FtsZ mutations that cause resistance to methicillin and TXA707, respectively.[107] The poor activity and absorption of new antibiotics targeting the thermally sensitive protein Z caused severe harm to the host flora.[101] Because of this, novel compounds that decrease medication resistance need to be identified and developed. The MD simulation-derived bending of helix H7 in FtsZ was confirmed by X-ray crystallography, which revealed two hidden pockets: BP1 (M49,

DOI: https://doi.org/10.70389/PJID.100006 | Premier Journal of Infectious Diseases 2026;6:100006

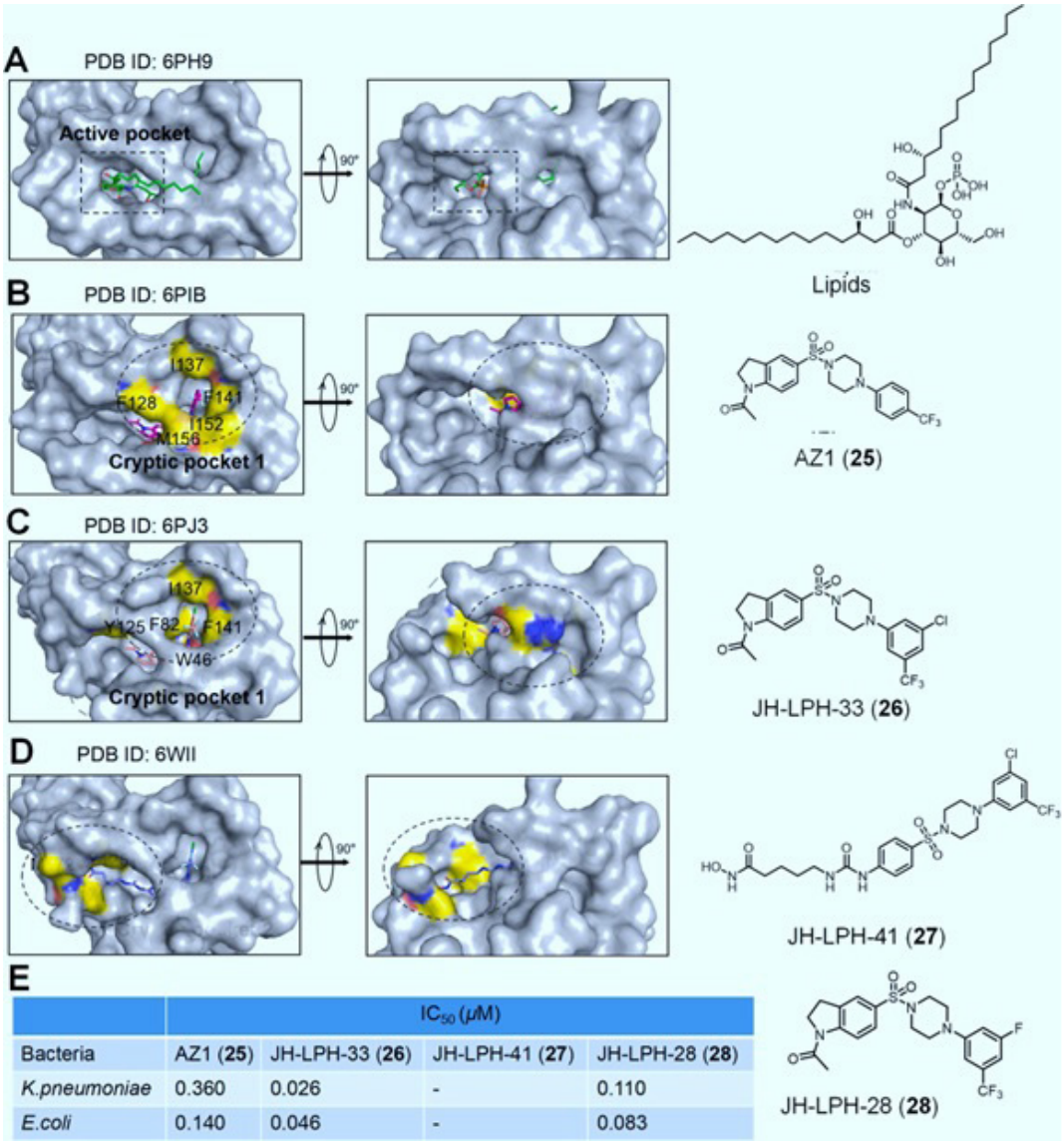

	IC_{50} (μM)			
Bacteria	AZ1 (**25**)	JH-LPH-33 (**26**)	JH-LPH-41 (**27**)	JH-LPH-28 (**28**)
K.pneumoniae	0.360	0.026	-	0.110
E.coli	0.140	0.046	-	0.083

Fig 6 | Finding inhibitors for UDP-diacylglucosamine pyrophosphohydrolase's cryptic pockets. The K. pneumoniae LpXH/Lid X, AZ1, JH-LPH-33, and JH-LPH-41 complexes are shown. AZ1, JH-LPH-28, JH-LPH-33, and JH-LPH-41 (E) inhibitor structures and IC_{50} values are shown

S50, and N25) and BP2 (E185, N189, E302, R304, and T306) (Figure 7A; Table 1).[108] The FtsZ function is inhibited by derivatives of coumarin (29 chemicals) and 4-hydroxycoumarin (30 compounds), with IC_{50} values of 200 μM (Figure 7B).[109] There is minimal affinity between the nucleotide-bound and 4-hydroxy analogue 30 forms of FtsZ. In addition, it establishes long-lasting links between BP1 and BP2. Extending electron density over the ligand, 30 oC entirely fills the pocket in BP1. Residues L47, M49, and D57 in the hydrophobic area of the binding cavity establish hydrophobic interactions with the benzyl group. The nitrogen atoms of K55 and S50's backbone nitrogen groups are joined by two hydrogen bonds in 4-hydroxycoumarin through carbonyl oxygens. In BP2, 30 is surrounded by G185, N189, Q192 (helix H7), I225 (strand β7), A262 (strand β7), E302, and R304 (strand β10). Figure 7B shows that, similar to BP1, the benzyl group forms hydrophobic interactions with E185, S227, G302, and R304, and that the 4-hydroxy group forms hydrogen bonds. Natural coumarin compounds binding to cryptic pockets decrease FtsZ polymerization and GTPase functions in 3D-QSAR screening, establishing a model for high-efficiency compound screening.[109] Therefore, delay of drug resistance can be achieved through compound creation with two cryptic pockets.

The cryptic binding pockets make it difficult to find drugs that target FtsZ to reduce its methicillin and TXA707 resistance. (1) Lack of structural data has hampered structure-based drug creation of a high-efficacy inhibitor. The binding conformation between FtsZ and compounds at the atomic level can guide compound structure modification, so drug design should focus on the two cryptic pockets and the active site simultaneously to delay drug resistance and increase FtsZ inhibitor selectivity.

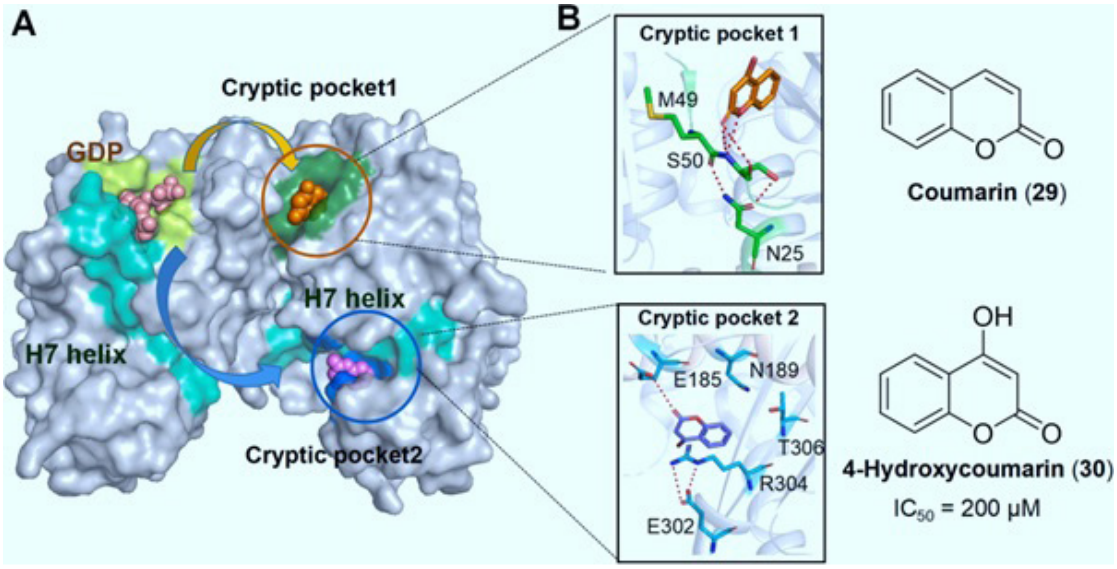

Fig 7 | Finding FtsZ cryptic pocket inhibitors. (A) FtsZ protein (PDB ID-6Y1U) attached to GDP (deep salmon sphere), 4-hydroxycoumarin in cryptic pockets 1 and 2 (orange and violet spheres), and the H7 helix. Cryptic pockets bind 4-hydroxycoumarin

Malate Dehydrogenase (MDH)

In addition to chloroplasts, the cytosol and glyoxysomes include perox isomes and MDH.[110] Functioning homeostasis requires the rapid conversion of malate into oxaloacetate, which requires NADH, and modification of the cytoplasmic NAD + /NADH ratio.[111] MDH controls the citric acid cycle, gluconeogenesis, metabolic stress, amino acid biosynthesis, oxidation/reduction equilibrium, and pathogens.[110] The dimer end of MDHs has a substrate-binding pocket, while the beginning has catalytic amino acid residues and a NAD-binding motif.[112] Stable MDH dimers have two functional domains. NAD+ or NADP+ catalyzes the irreversible conversion of malic acid into oxaloacetic acid in an MDH cleft.[113] MDH's active site binds the substrate and coenzyme's nicotinamide ring to produce a ternary complex. A protein's structure is altered by an external loop around the active site, catalyzing this vital activity.[113] The ABCB1 transporter may be triggered by MDH overexpression, releasing vinblastine, tariquidar, zosuquidar, colchicine, verapamil, and doxorubicin. This mechanism may boost ATP and produce resistance-associated proteins.[14] MDH increases cancer cell survival and prevents apoptosis by activating JNK. Previous research shows that prostate and uterine cancer cells can become docetaxel- and doxorubicin-resistant.[14,114] Clinical approval of MDH inhibitors is pending due to the lack of bacterial specificity in other active site medicines.[115] Discovery of cryptic areas increases the likelihood of finding MDH inhibitors that safely treat mycobacteria, S. aureus, E. coli, and other bacteria. High-throughput screening and X-ray scattering found MDH subsites 2 (G175-L177), 3 (Q211-M216), and 1 (L250, A272, K273, V282, and F284). Seven chemicals inhibited WT and V190W MDH in 1500 Maybridge library fragments tested by subsite 1 STD NMR. Only 4DT (31)[14,115] shows aromatic high-intensity peaks at 6 and 8 mg/L. Compound 31, with drug-like characteristics, inhibited MDH with a Kd of 99 μM and destabilized it with a △Tm of -2.00 ± 0.17 ◦C in MST tests. When we reached 31, the oligomeric interface's A and C chains were almost filled. It was 60% for chain A and 40% for chain C. V161, M200, F195, and F284 are side chain residues, and 31's sulfur atom has pocket van der Waals interactions. As shown in Figure 8A, the meta fluorine moiety engages the V169, V187, and N188 side chains. MDH's tetrameric structure remained intact after binding to 31; however, residues L250, V282, and K273 altered significantly in the A/D and B/C chains. Isopropyl derivatives induced steric effects, chlorine and bromine had high atomic radii, and nitrile had tri-fluoromethyl groups and electron-withdrawing effects. Fourb (35) and 7a (38), the two most potent 2 mM inhibitors, inhibited MDH activity by 80% and 77%, respectively, after 5a (36, 48%) and 5b (37, 47%). Compounds 1b (32, 40%), 2b (33, 35%), 4a (34, 35%), and 9a (39, 49%) inhibited MDH, unlike compound 31, which had low SO42 levels. The metaposition's trifluoromethyl group drastically reduced MDH's thermal stability, demonstrating that large functional groups can abolish it. 4DT compounds inhibited MDH non-competitively and lowered malate-binding affinity with different substrate concentrations.[116] High-throughput screening demonstrated that ZINC database chemicals CHLM, ACEE, ACTO, ETHR, ETOH, and CYPO strongly affected subsite 2. The majority of BIPH, ACET, CHLM, ACTO, DPME, and BENZ connected to subsite 3.[117] Since the host cytoplasm lacks similar cryptic sites, reasonably designed MDH agonists can target these sites (Table 1). The following issues need to be further studied, but lead drugs that target MDH's cryptic pockets have been identified: Most drugs work better at suppressing oligomeric and tetrameric MDH, which affects pathogen metabolic processes such as the citric acid cycle,

DOI: https://doi.org/10.70389/PJID.100006 | Premier Journal of Infectious Diseases 2026;6:100006

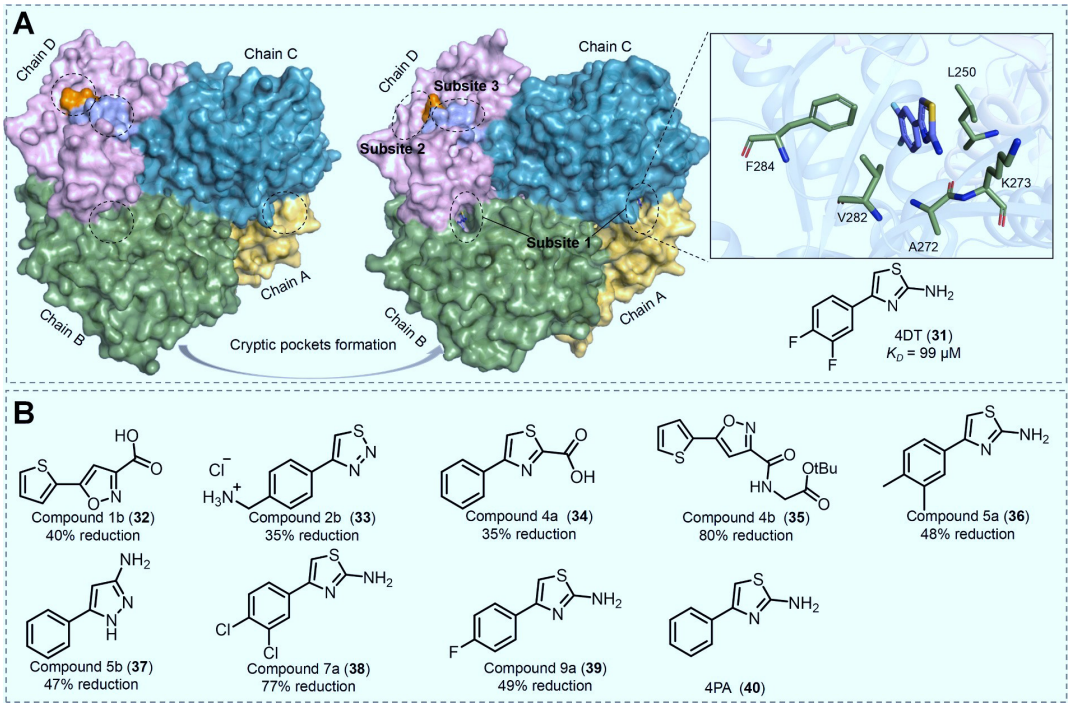

Fig 8 | Discovery of malate dehydrogenase cryptic pocket inhibitors. MDH's cryptic pockets (subsites 1, 2, and 3) and the discovery of compound 4DT based on subsite 1. Identification of Maybridge library chemicals targeting MDH1 subsite 1

gluconeogenesis, amino acid synthesis, etc. Low water solubility decreases bioavailability and complicates IC_{50} calculations for 4DT drugs. The inhibitory and selective actions of these chemicals must be understood to improve membrane permeability through structural alterations targeting molecules with higher affinity and modifying their physicochemical properties.

Antibiotic Modification/Biodegradation

Beta-Lactamase (β-Lactamase)

The four β-lactamase groups (A, B, C, and D) are mostly characterized by amino acid sequences in the BLA domain.[118] Some antibiotics depend on hydrolase β-lactamase. The serine moiety in the catalytic domain classifies β-lactamases as class A, C, or D. Due to zinc ions in their catalytic site, metallo-β-lactamases (MBLs) are classified as class B.[119] All pharmacologically licensed β-lactam antibiotics have a basic tetrameric azetidinone ring.[120] Gram-negative bacteria can produce β-lactamases, leading to resistance to β-lactam antibiotics. Carbapenem, cephalosporin, penicillin, and mono-bactam are less effective because these enzymes break the core four-membered azetidinone.[4] Gram-negative bacteria create β-lactamases in the periplasmic compartment, while Gram-positive bacteria create them in the cytoplasmic membrane. Different sites cause the two types of bacteria to break down β-lactam drugs differently.[121] Combining β-lactams with specific β-lactamase inhibitors can improve their effectiveness against β-lactamases.[122,123] In healthcare settings, azobactam, sulbactam, and clavulunate were the first β-lactamase inhibitors used.[124] The medications mostly targeted Class A β-lactamases, while Class D had varied inhibitory effects and Class B had no impact. In the past decade, β-lactam/β-lactamase inhibitors such ceftazidime/avibactam, meropenem/vaborbactam, and imipenem/relebactam have been used to treat drug-resistant infections.[125–127] Porin reduction or carbapenemase (class B and D) overexpression may make bacteria resistant to these drugs.[128] No class B β-lactam inhibitor medicines are currently approved for clinical studies. This limits hospital treatments for severe multidrug-resistant diseases.[129] Development of effective β-lactamase inhibitors, particularly for classes B and D, is crucial. Table 1 shows that TEM-1 and CTX-M-9 β-lactamases hydrolyze cefotaxime, and cryptic pockets can target them. Combined use of computational (MD simulation) and experimental (NMR) methods revealed the cryptic pockets of TEM-1 β-lactamase.[130,131] In Figure 9A, they are located between the Ω-loop pocket, helix H11 (271–289), and helix H10 (218–230). In 2004, a virtual screening found two compounds from the Maybridge library as candidate ligands for the TEM-1 β-lactamase cryptic pocket between helices 11 and 12. 3-(4-phenyl amino-phenylamino)-2-(1H-tetrazol-5-yl)-acrylonitrile and N,N-bis(4-chlorobenzyl) are compounds 1 and 2.1,H-indolyl tetraazol-5-amine. Residues 274–285 were shifted 1–3 Å from their apo locations, while residues 218–224 had α-carbon atoms displaced 3–7 Å, disrupting the secondary structure (Figure 9B).[132] 41 and 42 largely interacted with residues L221, L250, I279, and L286 (pocket walls) and I246, V261, and I263 (pocket foundation). The activity center was 16 Å from the contact point. Because these compounds change shape, substitution of R244 reduces catalytic activity. In typical β-lactam substrates, the residue

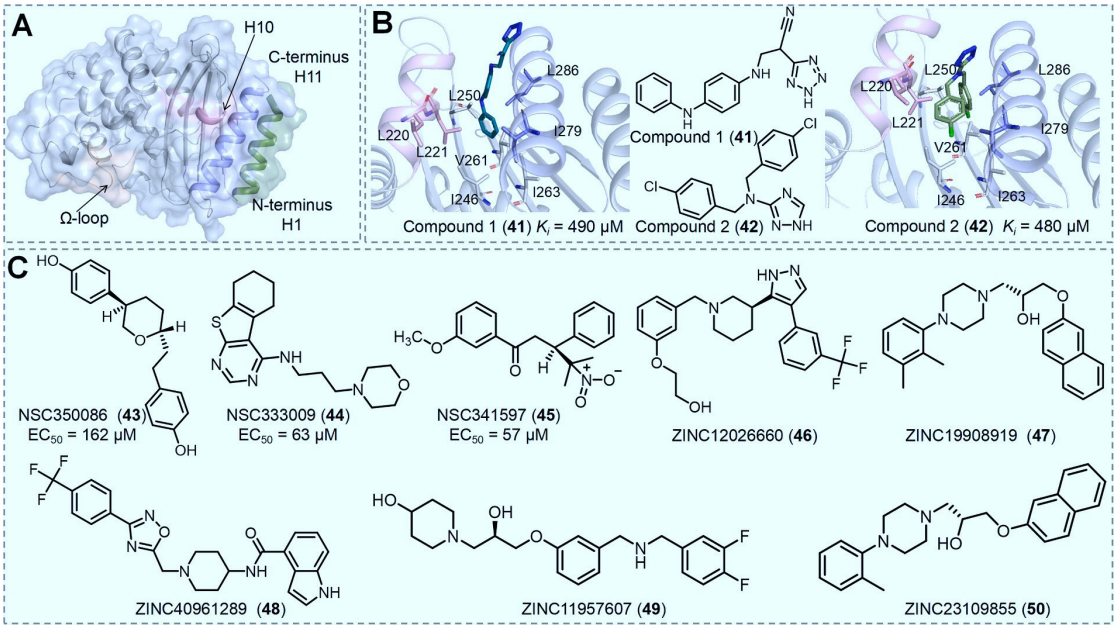

Fig 9 | Inhibitors targeting TEM-1 and CTX-M-9 β-lactamases' cryptic pocket were found. (A) Finding the elusive pockets (pocket 1) and Ω-loop (pocket 2) between H10 and H11 (PDB ID: 1BTL). (B) Compounds 1 (41) and 2 (42) bind to TEM-1 β-lactamase cryptic pocket 1 (PDB ID: 1PZO and 1PZP). High-throughput screening molecules bind cryptic pocket 1. The target bypass method

interacts with the C3′ carboxylate group. Both drugs suppressed wild-type TEM-1 β-lactamase and two mutants: M182T (480 μM and 460 μM) and G238A (590 μM and 590 μM). The NCI/DTP Open Chemical Repository improved compounds targeting the cryptic pocket between helices H10 and H11 by virtual screening. The activators and inhibitors were NSC350086 (43), NSC333009 (44), and NSC341597 (45).[133] All four 43 isomers, with an EC_{50} value of 162 μM, significantly increase nitrocefin catalytic efficiency (kcat/Km) by 52%. In Figure 9C, compound 44 increases kcat/Km by 52% at 162 μM EC_{50}, while compound 45 lowers it by 59% at 57 μM. TEM-1 β-lactamase catalytic activity was reduced by these three medications. 0.01% Triton-X inhibited 44 and 45 enzymes equally, suggesting that aggregation drives its non-selective mechanism. However, 43 did not work without Triton-X, validating a theory concerning its interaction with TEM and showing that its inclusion is necessary for 43's process. Mutation research demonstrates that the three chemical entities' alkyl chain portions form van der Waals bonds with L220, T265, and R 244. TEM-1 cryptic pockets require energy to open; thus, CYMAL-6 was added to aid detection. The chemical is the single TEM-1 inhibitor, with a Ki value of 40.05 μM and efficacy with 0.5 mM SDS.[134] Two CYMAL-6 and TEM-1 crystal structures exist. CYMAL-6's complex H bonds with H11C-terminal E280 and H10C-terminal V create similar complexes. Its cyclohexyl moiety and lengthy aliphatic amino acid sequence fit well in a hydrophobic pocket formed by A280, G283, I221, A268, and V261. primary structures (2A3U, 5EEB, 4ZAM, 4R3B, and 4MBF) had the cyclohexyl moiety from CYMAL-6 in their grooves, while secondary entities (1PZP, 1PZO) migrated away from H10 in the hydrophobic core. Next, half a million pounds from the ZINC database were high-throughput-screened. The highest Glide scores were reported in anisole (ZINC12026660 (46), ZINC19908919 (47), ZINC40961289 (48), and N-benzylacetamide derivatives). N-benzylacetamide and its anisole moieties were strategically positioned in the cyclohexyl segment of CYMAL-6, and the aromatic rings interact with R244 via pi–cation interactions. By targeting the cryptic pocket, natural humic substances may inhibit TEM-1. Only the coal humic acid (CHM) ethanol-soluble fraction from SHA, CHM, CHI, PHA, and CHP lowered TEM-1 catalysis by 42%. CHM may inhibit TEM-1 due to non-specific interaction between CHM compounds, the protein surface, and low-molecular-weight CHM constituents in the cryptic pocket, which affects the active site structure.[135] The only conserved Ω-loop cryptic site is found in TEM and CTX-M-9 β-lactamases.[131] Mutations (E240D/R241P) in the Ω-loop cryptic pocket indicate that pocket opening can increase benzylpenicillin activity, suggesting a potential therapeutic target. Using compounds that target cryptic pockets can minimize antibiotic resistance by reducing β-lactamase hydrolysis. Research on chemicals that target cryptic crevices in β-lactamases is crucial for modifying lead compounds' structures. Limitations exist in the use of cryptic pockets to tackle β-lactamase-induced antibiotic resistance: (1) Improving TEM-1 β-lactamase cryptic pocket inhibitor binding and efficacy; (2) testing Ω-loop drug design for efficacy; and (3) evaluating synergistic effects of active and cryptic pocket inhibitors. This method can combat antibiotic resistance and identify inhibitors in class B, C, and D β-lactamases. This can hinder the degradation of β-lactam medicines by various β-lactamases.

DOI: https://doi.org/10.70389/PJID.100006 | Premier Journal of Infectious Diseases 2026;6:100006

Disulfide-Bond-Forming Protein A (DsbA)

DsbA controls protein folding, efficiency, and secreted state integrity.[136] Periplasmic synthesis affects extracellular proteins and multimeric cell surface structures.[137] Failure to synthesize enough DsbA causes protein misfolding and emergence of harmless microorganisms.[136] DsbA has known helical sections and a TRX domain.[138] The structure of the TRX domain resembles disulfide oxidoreductases, featuring four β-strands and two α-helices (β4β5β6 and β2α1β3 motifs). DsbA's active site contains the TRX domain's conserved CXXC motif (C30-F31-H32-C33).[139] The low-pKa reduced thioalte ion C30 is stabilized by hydrogen bonding with carbon atoms C33 (thiol) and H32 (backbone amide nitrogens).[140,141] A TRX domain cis-proline loop aids substrate binding and thioredoxin fold protein redox modification.[142,143] The broad hydrophobic helical domain above the active site interacts with substrates to stabilize and select substrate binding.[144] "Target bypassing," which favors pathogenic virulence over viability, reduces antibiotic resistance.[145] Antibiotic resistance can be reduced by targeting virulence modulator DsbA.[146] However, existing DsbA inhibitors require a cysteine mutation to interact with the active site.[147,148] Novel DsbA pockets may enable the formation of non-covalent inhibitors. X-ray crystallography and NMR investigations showed that reorienting Y110 in DsbA resulting in the formation of the cryptic pocket (Y110, L112). In 2021, the Monash Institute for Pharmaceutical Science (MIPS) fragment libraries were used for ligand-detected saturation-transfer difference (STD) NMR high-throughput screening of 1,130 fragments for DsbA's cryptic pocket (Figure 10A; Table 1).[15] Bromophenoxy propanamide (fragment 1 (51)) and 4-methoxy-N-phenylbenzenesulfonamide (fragment 2 (52)) were chosen because they preferentially bind with BpsDsbA's oxidized catalytic region (Figure 10B). The crystal structures of the symmetry-related protein showed V12, A13, and K15, while 51 hydrophobically interacted with the secondary moieties of Y110, W40, F77, and L112 in the original protein. The aromatic rings of 51 and Y110 had π-stacking interactions within 10 Å of the redox active-site residue C43. The fragments likely inhibited DsbA (Kd > 2 mM) due to their tiny surface areas and partial pocket occupancy. A fluorescently tagged synthetic peptide with cysteines or fragments reduced the BpsDsbA–BpsDsbB redox cycle at 20 mM in a peptide-oxidation experiment. These results showed that peptides 51 and 52 lacked the binding affinity to inhibit or compete with BpsDsbA. However, these compounds may improve DsbA-binding molecules. DsbA's cryptic pocket may lead to the formation of effective inhibitors via structural derivations and optimization of 51 and 52. In vivo testing to determine if the inhibitor kills DsbA bacteria is also needed. The close proximity of the cryptic and active sites suggests that drugs binding to both pockets can synergistically suppress pathogens.

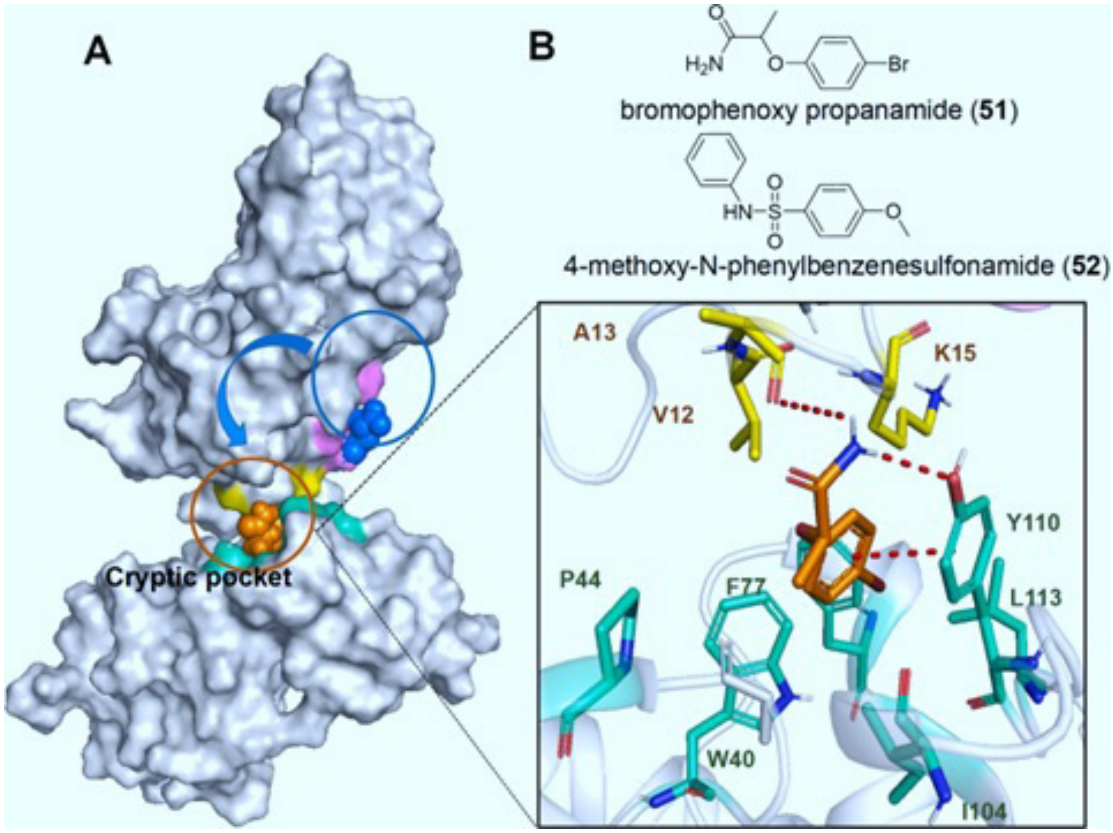

Fig 10 | Discovery of DsbA cryptic pocket inhibitors. DsbA–bromophenoxy propanamide structure in the cryptic pocket (orange sphere). (B) Bromophenoxy propanamide–cryptic pocket interactions

Conclusion and Perspective

As 46.5% of antibiotic targets are resistant, microorganism resistance is common. Cryptic inhibitors may cure antibiotic-resistant diseases. In 5.3% of drug-resistant proteins, cryptic pocket inhibitors work. It is difficult to find and use cryptic niches to fight antibiotic resistance. This study explored antibiotic resistance, cryptic pockets' involvement in lowering resistance, and the interaction between cryptic pockets, tiny molecular inhibitors, and eight antibiotic targets (β-lactamase, HPPK, LpxH, FP-2, MDH, DHPS, FtsZ, and DsbA). We can forecast and detect complex cryptic pockets using computational and experimental methods. Cryptic pocket identification now has an accurate, easy-to-use computational foundation. The lack of fully sampled spatial simulations and protein motions hinders crypto pocket prediction in long protein chains. Future investigations will need to choose training data sets after collecting accurate data. Machine learning and deep learning must balance forecast accuracy with efficiency. High-throughput screening, cysteine capture, and thiol labeling can result in wastage of time and resources on false negatives. These protein molecular weight and structure problems restrict the development of superior NMR and X-ray technologies for every protein. Cryptic pocket identification can be improved by AI models and computations, and flexible experimental methods. Despite high-throughput screening and fragment-based rational drug design, there has been no advancement in small-molecule inhibitors for cryptic pockets. The ligand's lumen occupancy time affects these methods' efficacy, which can cause off-target consequences from binding to other targets. Unreliable screening databases and scaffolds limit cryptic pocket inhibitor application. We suggest collecting important data on cryptic pocket inhibitors and using them in a structured database to build lead compounds that block them. Cryptic antibiotic ligands are structurally diverse, synergistic, and non-cross-resistant. Because antibiotics targeting cryptic pockets modify protein function differently, cryptic site ligands are unlikely to develop resistance to active site medications. Second, active site and cryptic antibiotics inhibit protein activation. Inhibitors that target protein double pockets may reduce medicine resistance. Third, cryptic pockets provide for structural diversity in medications and novel antibacterial compositions. Due to their structural variety, lack of cross-resistance, and synergistic efficacy, cryptic pocket antibiotics may delay drug resistance. The low fitness cost, drugability, and mechanism of action of cryptic site ligands hamper the creation of new antibiotics. Unlike active sites, cryptic pockets have less visible architecture and no "hot spot" residues; therefore, medicines target them less. Second, proteins with cryptic pocket mutations act or function similarly, suggesting that they may not increase fitness burden, since cryptic pockets are remote from functional regions. Cryptic site ligands alone could produce antibiotic resistance. Third, the mechanism by which antibiotics fight microorganisms is unknown. Medications that target cryptic pockets may modify functional site architecture and downstream signaling to fight bacterial infections. Thus, future research should examine cryptic pocket protein crystal structure, application tactics (combined with active site-binding medicines), and downstream control mechanisms.

References

1 Jeukens J, Freschi L, Kukavica-Ibrulj I, Emond-Rheault JG, Tucker NP, Levesque RC. Genomics of antibiotic-resistance prediction in *Pseudomonas aeruginosa*. *Ann NY Acad Sci*. 2019;1435(1):5–17. https://doi.org/10.1111/nyas.13358

2 Bylander J. Superbugs: an arms race against bacteria. *Health Aff*. 2019;38(4):692–692.

3 Ahmed SK, Hussein S, Qurbani K, et al. Antimicrobial resistance: impacts, challenges, and future prospects. *J Med Surg Public Health*. 2024;2:100081. https://doi.org/10.1016/j.glmedi.2024.100081

4 Lima LM, Silva B, Barbosa G, Barreiro EJ. β-lactam antibiotics: an overview from a medicinal chemistry perspective. *Eur J Med Chem*. 2020;208:112829. https://doi.org/10.1016/j.ejmech.2020.112829

5 Williams JD. Beta-lactamases and beta-lactamase inhibitors. *Int J Antimicrob Agents*. 1999;12(1):S3–S7, discussion S26-7.

6 Lima LM, Md Silva BN, Barbosa G, Barreiro EJ. β-lactam antibiotics: an overview from a medicinal chemistry perspective. *Eur J Med Chem*. 2020;208:112829. https://doi.org/10.1016/j.ejmech.2020.112829

7 Gao YY, Yang WC, Ashby CR, Hao GF. Mapping cryptic binding sites of drug targets to overcome drug resistance. *Drug Resist Updat*. 2023;67:100934. https://doi.org/10.1016/j.drup.2023.100934

8 Vajda S, Beglov D, Wakefield AE, Egbert M, Whitty A. Cryptic binding sites on proteins: definition, detection, and druggability. *Curr Opin Chem Biol*. 2018;44:1–8. https://doi.org/10.1016/j.cbpa.2018.05.003

9 Yun MK, Hoagland D, Kumar G, et al. The identification, analysis and structure-based development of novel inhibitors of 6-hydroxymethyl-7,8-dihydropterin pyrophosphokinase. *Bioorg Med Chem*. 2014;22(7):2157–2165. https://doi.org/10.1016/j.bmc.2014.02.022

10 Cho J, Lee M, Cochrane CS, et al. Structural basis of the UDP-diacylglucosamine pyrophosphohydrolase LpxH inhibition by sulfonyl piperazine antibiotics. *Proc Natl Acad Sci U S A*. 2020;117(8):4109–4116. https://doi.org/10.1073/pnas.1912876117

11 Hernández JE, González, Salas-Sarduy E, Hernández Alvarez L, et al. In silico identification of noncompetitive inhibitors targeting an uncharacterized allosteric site of falcipain-2. *J Comput Aided Mol Des*. 2021;35(10):1067–1079. https://doi.org/10.1007/s10822-021-00420-7

12 Hammoudeh DI, Dáte M, Yun M-K, et al. Identification and characterization of an allosteric inhibitory site on dihydropteroate synthase. *ACS Chem Biol*. 2014;9(6):1294–1302. https://doi.org/10.1021/cb500038g

13 Duggirala S, Nankar RP, Rajendran S, Doble M. Phytochemicals as inhibitors of bacterial cell division protein FtsZ: coumarins are promising candidates. *Appl Biochem Biotechnol*. 2014;174(1):283–296. https://doi.org/10.1007/s12010-014-1056-2

14 Lo YW, Lin ST, Chang SJ, et al. Mitochondrial proteomics with siRNA knock down to reveal ACAT1 and MDH2 in the development of doxorubicin-resistant uterine cancer. *J Cell Mol Med*. 2015;19(4):744–759. https://doi.org/10.1111/jcmm.12388

15 Petit GA, Mohanty B, McMahon RM, et al. Identification and characterization of two drug-like fragments that bind to the same cryptic binding pocket of Burkholderia pseudomallei DsbA. *Acta Crystallogr D Struct. Biol*. 2022;78(Pt 1):75–90. https://doi.org/10.1107/S2059798321011475

16 Dennis ML, Pitcher NP, Lee MD, et al. Structural basis for the selective binding of inhibitors to 6-hydroxymethyl-7,8-dihydropterin pyrophosphokinase from *Staphylococcus aureus* and *Escherichia coli*. *J Med Chem*. 2016;59(11):5248–5263. https://doi.org/10.1021/acs.jmedchem.6b00002

17 Nayar AS, Dougherty TJ, Ferguson KE, et al. Novel antibacterial targets and compounds revealed by a high-throughput cell wall reporter assay. *J Bacteriol*. 2015;197(10):1726–1734. https://doi.org/10.1128/JB.02552-14

18 Kapoor G, Saigal S, Elongavan A. Action and resistance mechanisms of antibiotics: a guide for clinicians. *J Anaesthesiol Clin Pharmacol*. 2017;33(3):300–305. https://doi.org/10.4103/joacp.JOACP_349_15

19 Brooks BD, Brooks AE. Therapeutic strategies to combat antibiotic resistance. *Adv Drug Deliv Rev*. 2014;78:14–27. https://doi.org/10.1016/j.addr.2014.10.027

20 Nabadda S, Kakooza F, Kiggundu R, et al. Implementation of the World Health Organization Global Antimicrobial Resistance Surveillance System in Uganda, 2015–2020: mixedmethods study using national surveillance data. *JMIR Public Health Surveill*. 2021;7(10). https://doi.org/10.2196/29954

21 Luo Q, Lu P, Chen Y, et al. ESKAPE in China: epidemiology and characteristics of antibiotic resistance. *Emerg Microbes Infect*. 2024;13(1):2317915. https://doi.org/10.1080/22221751.2024.2317915

22 Hu F, Pan Y, Li H, et al. Carbapenem-resistant *Klebsiella pneumoniae* capsular types, antibiotic resistance and virulence factors in China: a longitudinal, multi-centre study. *Nat Microbiol*. 2024;9(3):814–829. https://doi.org/10.1038/s41564-024-01612-1

23 Mat Rahim N, Lee H, Strych U, AbuBakar S. Facing the challenges of multidrugresistant *Acinetobacter baumannii*: progress and prospects in the vaccine development. *Hum Vaccin Immunother*. 2021;17(10):3784–3794. https://doi.org/10.1080/21645515.2021.1927412

24 Davis BC, Keenum I, Calarco J, et al. Towards the standardization of Enterococcus culture methods for waterborne antibiotic resistance monitoring: a critical review of trends across studies. *Water Res X*. 2022;17:100161. https://doi.org/10.1016/j.wroa.2022.100161

25 Ogawara H. Comparison of antibiotic resistance mechanisms in antibioticproducing and pathogenic bacteria. *Molecules*. 2019;24(19):3430. https://doi.org/10.3390/molecules24193430

26 Darby EM, Trampari E, Siasat P, et al. Molecular mechanisms of antibiotic resistance revisited. *Nat Rev Microbiol*. 2023;21(5):280–295. https://doi.org/10.1038/s41579-022-00820-y

27 Then RL. Mechanisms of resistance to trimethoprim, the sulfonamides, and trimethoprim-sulfamethoxazole. *Rev Infect Dis*. 1982;4(2):261–269. https://doi.org/10.1093/clinids/4.2.261

28 Munita JM, Arias CA. Mechanisms of antibiotic resistance. *Microbiol Spectr*. 2016;4(2) https://doi.org/10.1128/microbiolspec.VMBF-0016-2015

29 Stapleton PD, Taylor PW. Methicillin resistance in *Staphylococcus aureus*: mechanisms and modulation. *Sci Prog*. 2002;85(Pt 1):57–72. https://doi.org/10.3184/003685002783238870

30 Méndez-Alvarez S, Pérez-Hernández X, Claverie-Martín F. Glycopeptide resistance in enterococci. *Int Microbiol*. 2000;3(2):71–80.

31 Miller WR, Munita JM, Arias CA. Mechanisms of antibiotic resistance in enterococci. *Expert Rev Anti Infect Ther*. 2014;12(10):1221–1236. https://doi.org/10.1586/14787210.2014.956092

32 Jiang M, Su YB, Ye JZ, et al. Ampicillin-controlled glucose metabolism manipulates the transition from tolerance to resistance in bacteria. 2023;9(10):eade8582. https://doi.org/10.1126/sciadv.ade8582

33 Blair JM, Webber MA, Baylay AJ, Ogbolu DO, Piddock LJ. Molecular mechanisms of antibiotic resistance. *Nat Rev Microbiol*. 2015;13(1):42–51. https://doi.org/10.1038/nrmicro3380

34 Billal DS, Feng J, Leprohon P, Legare D, Ouellette M. Whole genome analysis of linezolid resistance in *Streptococcus pneumonia*e reveals resistance and compensatory mutations. *BMC Genomics*. 2011;12:512. https://doi.org/10.1186/1471-2164-12-512

35 Gao W, Chua K, Davies JK, et al. Two novel point mutations in clinical *Staphylococcus aureus* reduce linezolid susceptibility and switch on the stringent response to promote persistent infection. *PLoS Pathog*. 2010;6(6):e1000944. https://doi.org/10.1371/journal.ppat.1000944

36 Leclercq R. Mechanisms of resistance to macrolides and lincosamides: nature of the resistance elements and their clinical implications. *Clin Infect Dis*. 2002;34(4):482–492. https://doi.org/10.1086/324626

37 Unemo M, Golparian D, Nicholas R, Ohnishi M, Gallay A, Sednaoui P. Highlevel cefixime- and ceftriaxone-resistant Neisseria gonorrhoeae in France: novel penA mosaic allele in a successful international clone causes treatment failure. *Antimicrob. Agents Chempther*. 2012;56(3):1273–1280. https://doi.org/10.1128/AAC.05760-11

38 Schaenzer AJ, Wright GD. Antibiotic resistance by enzymatic modification of antibiotic targets. *Trends Mol Med*. 2020;26(8):768–782. https://doi.org/10.1016/j.molmed.2020.05.001

39 Lambert PA. Bacterial resistance to antibiotics: modified target sites. *Adv Drug Deliv Rev*. 2005;57(10):1471–1485. https://doi.org/10.1016/j.addr.2005.04.003

40 Dzyubak E, Yap MNF. The expression of antibiotic resistance methyltransferase correlates with mRNA stability independently of ribosome stalling. *Antimicrob Agents Chemother*. 2016;60(12):7178–7188. https://doi.org/10.1128/AAC.01806-16

41 Long KS, Poehlsgaard J, Kehrenberg C, Schwarz S, Vester B. The Cfr rRNA methyltransferase confers resistance to Phenicols, Lincosamides, Oxazolidinones, Pleuromutilins, and Streptogramin A antibiotics. *Antimicrob Agents Chemother*. 2006;50(7):2500–2505. https://doi.org/10.1128/AAC.00131-06

42 Webber MA, Piddock LJ. The importance of efflux pumps in bacterial antibiotic resistance. *J Antimicrob Chemother*. 2003;51(1):9–11. https://doi.org/10.1093/jac/dkg050

43 Guilfoile PG, Hutchinson CR. A bacterial analog of the mdr gene of mammalian tumor cells is present in Streptomyces peucetius, the producer of daunorubicin and doxorubicin. *Proc Natl Acad Sci U S A*. 1991;88(19):8553–8557. https://doi.org/10.1073/pnas.88.19.8553

44 Li W, Sharma M, Kaur P. The DrrAB efflux system of Streptomyces peucetius is a multidrug transporter of broad substrate specificity. *J Biol Chem*. 2014;289(18):12633–12646. https://doi.org/10.1074/jbc.M113.536136

45 Veal WL, Nicholas RA, Shafer WM. Overexpression of the MtrC-MtrD-MtrE efflux pump due to an mtrR mutation is required for chromosomally mediated penicillin resistance in Neisseria gonorrhoeae. *J Bacteriol*. 2002;184:5619–5624. https://doi.org/10.1128/JB.184.20.5619-5624.2002

46 Chen SC, Connolly KL, Rouquette-Loughlin C, D'Andrea A, Jerse AE, Shafer WM. Could dampening expression of the Neisseria gonorrhoeae mtrCDEencoded efflux pump be a strategy to preserve currently or resurrect formerly used antibiotics to treat gonorrhea? *mBio*. 2019;10(4):e01576–19. https://doi.org/10.1128/mBio.01576-19

47 Wind CM, de Vries E, Schim van der Loeff MF, et al. Decreased azithromycin susceptibility of Neisseria gonorrhoeae isolates in patients recently treated with azithromycin. *Clin Infect Dis*. 2017;65(1):37–45. https://doi.org/10.1093/cid/cix249

48 Forsberg KJ, Patel S, Wencewicz TA, Dantas G. The tetracycline destructases: a novel family of tetracycline-inactivating enzymes. *Chem Biol*. 2015;22(7):888–897. https://doi.org/10.1016/j.chembiol.2015.05.017

49 Livermore DM. Defining an extended-spectrum beta-lactamase. *Clin Microbiol Infect*. 2008;14(1):3–10. https://doi.org/10.1111/j.1469-0691.2007.01857.x

50 Nordmann P, Poirel L, Walsh TR, Livermore DM. The emerging NDM carbapenemases. *Trends Microbiol*. 2011;19(12):588–595. https://doi.org/10.1016/j.tim.2011.09.005

51 Voulgari E, Poulou A, Koumaki V, Tsakris A. Carbapenemase-producing Enterobacteriaceae: now that the storm is finally here, how will timely detection help us fight back? *Future Microbiol*. 2013;8(1):27–39. https://doi.org/10.2217/fmb.12.130

52 Woodford N, Turton JF, Livermore DM. Multiresistant gram-negative bacteria: the role of high-risk clones in the dissemination of antibiotic resistance. *FEMS Microbiol Rev*. 2011;35(5):736–755. https://doi.org/10.1111/j.1574-6976.2011.00268.x

53 Fang LX, Chen C, Cui CY, et al. Emerging high-level tigecycline resistance: novel tetracycline destructases spread via the mobile tet(x). *BioEssays* 2020;42(8):e2000014. https://doi.org/10.1002/bies.202000014

54 Peterson E, Kaur P. Antibiotic resistance mechanisms in bacteria: relationships between resistance determinants of antibiotic producers, environmental bacteria, and clinical pathogens. *Front Microbiol*. 2018;9, https://doi.org/10.3389/fmicb.2018.02928

55 Sugiyama M, Kumagai T, Matsuo H, et al. Overproduction of the bleomycin-binding proteins from bleomycin-producing Streptomyces verticillus and a methicillin-resistant *Staphylococcus aureus* in Escherichia coli and their immunological characterisation. *FEBS Lett*. 1995;362(1):80–84. https://doi.org/10.1016/0014-5793(95)00218-X

56 Rudolf JD, Bigelow L, Chang C, et al. Crystal structure of the Zorbamycin-binding protein ZbmA, the primary self-resistance element in Streptomyces flavoviridis ATCC21892. *Biochemistry*. 2015;54(45):6842–6851. https://doi.org/10.1021/acs.biochem.5b01008

57 Gatignol A, Durand H, Tiraby G. Bleomycin resistance conferred by a drugbinding protein. *FEBS Lett*. 1988;230(1-2):171–175.

58 Sugiyama M, Kumagai T. Molecular and structural biology of bleomycin and its resistance determinants. *J Biosci Bioeng*. 2002;93(2):105–116. https://doi.org/10.1016/S1389-1723(02)80001-9

59 Chang CY, Yan XH, Crnovcic I, et al. Resistance to enediyne antitumor antibiotics by sequestration. *Cell Chem Biol*. 2018;25(9):1075–1075. https://doi.org/10.1016/j.chembiol.2018.05.012

60 Zhao XL, Chen ZG, Yang TC, et al. Glutamine promotes antibiotic uptake to kill multidrug-resistant uropathogenic bacteria. *Sci Transl Med*. 2021;13(625):eabj0716. https://doi.org/10.1126/scitranslmed.abj0716

61 Cimermancic P, Weinkam P, Rettenmaier TJ, et al. CryptoSite: expanding the druggable proteome by characterization and prediction of cryptic binding sites. *J Mol Biol*. 2016;428(4):709–719. https://doi.org/10.1016/j.jmb.2016.01.029

62 Laskowski RA, Gerick F, Thornton JM. The structural basis of allosteric regulation in proteins. *FEBS Lett*. 2009;583(11):1692–1698. https://doi.org/10.1016/j.febslet.2009.03.019

63 Oleinikovas V, Saladino G, Cossins BP, Gervasio FL. Understanding cryptic pocket formation in protein targets by enhanced sampling simulations. *J Am Chem Soc*. 2016;138(43):14257–14263. https://doi.org/10.1021/jacs.6b05425

64 Beglov D, Hall DR, Wakefield AE, et al. Exploring the structural origins of cryptic sites on proteins. *Proc Natl Acad Sci U S A*. 2018;115(15):3416–3425. https://doi.org/10.1073/pnas.1711490115

65 Shi G, Gong Y, Savchenko A, et al. Dissecting the nucleotide binding properties of Escherichia coli 6-hydroxymethyl-7,8-dihydrop terin pyrophosphokinase with fluorescent 3′(2)′-o-anthraniloyladenosine 5′-triphosphate. *Biochim Biophys Acta*. 2000;1478(2):289–299. https://doi.org/10.1016/S0167-4838(00)00043-1

66 Toulouse JL, Shi G, Lemay-St-Denis C, et al. Dual-target inhibitors of the folate pathway inhibit intrinsically trimethoprim-resistant DfrB dihydrofolate reductases. *ACS Med Chem Lett*. 2020;11(11):2261–2267. https://doi.org/10.1021/acsmedchemlett.0c00393

67 Maynard C, Cummins I, Green J, Weinkove D. A bacterial route for folic acid supplementation. *BMC Biol*. 2018;16(1):67. https://doi.org/10.1186/s12915-018-0534-3

68 Yan H, Blaszczyk J, Xiao B, Shi G, Ji X. Structure and dynamics of 6-hydrox ymethyl-7,8-dihydropterin pyrophosphokinase. *J Mol Graph Model*. 2001;19(1):70–77. https://doi.org/10.1016/S1093-3263(00)00135-2

69 Teichmann SA, Murzin AG, Chothia C. Determination of protein function, evolution and interactions by structural genomics. *Curr Opin Struct Biol*. 2001;11(3):354–363. https://doi.org/10.1016/S0959-440X(00)00215-3

70 Xiao B, Shi G, Gao J, et al. Unusual conformational changes in 6-Hydroxymethyl-7,8-dihydropterin pyrophosphokinase as revealed by X-ray crystallography and NMR*. *J Biol Chem*. 2001;276(43):40274–40281. https://doi.org/10.1074/jbc.M103837200

71 Blaszczyk J, Shi G, Li Y, Yan H, Ji X. Reaction trajectory of pyrophosphoryl transfer catalyzed by 6-hydroxymethyl-7,8-dihydropterin pyrophosphokinase. *Structure*. 2004;12(3):467–475. https://doi.org/10.1016/j.str.2004.02.003

72 Blaszczyk J, Li Y, Wu Y, Shi G, Ji X, Yan H. Essential roles of a dynamic loop in the catalysis of 6-hydroxymethyl-7,8-dihydropterin pyrophosphokinase. *Biochemistry*. 2004;43(6):1469–1477. https://doi.org/10.1021/bi036053l

73 Yun MK, Hoagland D, Kumar G, et al. The identification, analysis and structure-based development of novel inhibitors of 6-hydroxymethyl-7,8-dihydropterin pyrophosphokinase. *Bioorg Med Chem*. 2014;22(7):2157–2165. https://doi.org/10.1016/j.bmc.2014.02.022

74 Zhao LC, Lu HP, Wang J. Exploration of multistate conformational dynamics upon ligand binding of a monomeric enzyme involved in pyrophosphoryl transfer. *J Phys Chem B*. 2018;122(6):1885–1897. https://doi.org/10.1021/acs.jpcb.7b12562

75 Schneider G. Virtual screening: an endless staircase? *Nat Rev Drug Discov*. 2010;9(4):273–276. https://doi.org/10.1038/nrd3139

76 Valderas MW, Andi B, Barrow WW, Cook PF. Examination of intrinsic sulfonamide resistance in Bacillus anthracis: a novel assay for dihydropteroate synthase. *Biochim Biophys Acta*. 2008;1780(5):848–853. https://doi.org/10.1016/j.bbagen.2008.02.003

77 Stratton CF, Namanja-Magliano HA, Cameron SA, Schramm VL. Binding isotope effects for para-aminobenzoic acid with dihydropteroate synthase from *Staphylococcus aureus* and *Plasmodium falciparum*. *ACS Chem Biol*. 2015;10(10):2182–2186. https://doi.org/10.1021/acschembio.5b00490

78 Dosselaere F, Vanderleyden J. A metabolic node in action: chorismate-utilizing enzymes in microorganisms. *Crit Rev Microbiol*. 2001;27(2):75–131. https://doi.org/10.1080/20014091096710

79 Vadlamani G, Sukhoverkov KV, Haywood J, et al. Crystal structure of Arabidopsis thaliana HPPK/DHPS, a bifunctional enzyme and target of the herbicide asulam. *Plant Commun*. 2022;3(4):100322. https://doi.org/10.1016/j.xplc.2022.100322

80 Guo J-s, Liu K-l, Qin Y-x, et al. Hypusinationinduced DHPS/eIF5A pathway as a new therapeutic strategy for human diseases: a mechanistic review and structural classification of DHPS inhibitors. *Biomed. Pharmacother*. 2023;167:115440. https://doi.org/10.1016/j.biopha.2023.115440

81 Achari A, Somers DO, Champness JN, Bryant PK, Rosemond J, Stammers DK. Crystal structure of the anti-bacterial sulfonamide drug target dihydropteroate synthase. *Nat Struct Biol*. 1997;4(6):490–497. https://doi.org/10.1038/nsb0697-490

82 Mondal S, Malakar S. Synthesis of sulfonamide and their synthetic and therapeutic applications: recent advances. *Tetrahedron*. 2020;76(48):131662. https://doi.org/10.1016/j.tet.2020.131662

83 Barnadas C, Musset L, Legrand E, et al. Short report: high prevalence and fixation of *Plasmodium vivax* dhfr/dhps mutations related to sulfadoxine/pyrimethamine resistance in french guiana. *Am J Trop Med Hyg*. 2009;81(1):19–22. https://doi.org/10.4269/ajtmh.2009.81.19

84 Hammoudeh DI, Zhao Y, White SW, Lee RE. Replacing sulfa drugs with novel DHPS inhibitors. *Future Med Chem*. 2013;5(11):1331–1340. https://doi.org/10.4155/fmc.13.97

85 Heidari A, Dittrich S, Jelinek T, Kheirandish A, Banihashemi K, Keshavarz H. Genotypes and in vivo resistance of *Plasmodium falciparum* isolates in an endemic region of Iran. *Parasitol Res*. 2007;100(3):589–592. https://doi.org/10.1007/s00436-006-0291-z

86 Zhao Y, Hammoudeh D, Yun MK, Qi JJ, White SW, Lee RE. Structure-based design of novel pyrimido[4,5-c]pyridazine derivatives as dihydropteroate synthase inhibitors with increased affinity. *ChemMedChem* 2012;7(5):861–870. https://doi.org/10.1002/cmdc.201200049

87 Wang XY, Quinn PJ. Lipopolysaccharide: biosynthetic pathway and structure modification. *Prog Lipid Res*. 2010;49(2):97–107. https://doi.org/10.1016/j.plipres.2009.06.002

88 Cho J, Lee CJ, Zhao JS, Young HE, Zhou P. Structure of the essential *Haemophilus influenzae* UDP-diacylglucosamine pyrophosphohydrolase LpxH in lipid A biosynthesis. *Nat Microbiol*. 2016;1(11):16154. https://doi.org/10.1038/nmicrobiol.2016.154

89 Garcia-Vello P, Di Lorenzo F, Zucchetta D, Zamyatina A, De Castro C, Molinaro A. Lipopolysaccharide lipid A: a promising molecule for new immunitybased therapies and antibiotics. *Pharmacol Ther*. 2022;230:107970. https://doi.org/10.1016/j.pharmthera.2021.107970

90 Cho J, Lee M, Cochrane CS, et al. Structural basis of the UDP-diacylglucosamine pyrophosphohydrolase LpxH inhibition by sulfonyl piperazine antibiotics. *Proc Natl Acad Sci U S A*. 2020;117(8):4109–4116. https://doi.org/10.1073/pnas.1912876117

91 Zhou P, Hong JY. Structure- and ligand-dynamics-based design of novel antibiotics targeting lipid A enzymes LpxC and LpxH in gram-negative bacteria. *Acc Chem Res*. 2021;54(7):1623–1634. https://doi.org/10.1021/acs.accounts.0c00880

92 Okada C, Wakabayashi H, Kobayashi M, Shinoda A, Tanaka I, Yao M. Crystal structures of the UDP-diacylglucosamine pyrophosphohydrase LpxH from *Pseudomonas aeruginosa*. *Sci Rep*. 2016;6:32822. https://doi.org/10.1038/srep32822

93 Kwak SH, Cochrane CS, Ennis AF, et al. Synthesis and evaluation of sulfonyl piperazine LpxH inhibitors. *Bioorg Chem*. 2020;102:104055. https://doi.org/10.1016/j.bioorg.2020.104055

94 Zhou P, Zhao JS. Structure, inhibition, and regulation of essential lipid A enzymes. *Biochim Biophys Acta Mol Cell Biol Lipids*. 2017;1862(11):1424–1438. https://doi.org/10.1016/j.bbalip.2016.11.014

95 Young HE, Donohue MP, Smirnova TI, Smirnov AI, Zhou P. The UDPdiacylglucosamine pyrophosphohydrolase LpxH in lipid A biosynthesis utilizes Mn2+ cluster for catalysis. *J Biol Chem*. 2013;288(38):26987–27001. https://doi.org/10.1074/jbc.M113.497636

96 Kwak S-H, Skyler Cochrane C, Cho J, et al. Development of LpxH inhibitors chelating the active site dimanganese metal cluster of LpxH. *ChemMedChem* 2023;18(11):e202300023.

97 Lee M, Zhao JS, Kwak SH, et al. Structure-activity relationship of sulfonyl piperazine LpxH inhibitors analyzed by an LpxE-coupled malachite green assay. *ACS Infect Dis*. 2019;5(4):641–651. https://doi.org/10.1021/acsinfecdis.8b00364

98 Han HH, Wang ZL, Li T, et al. Recent progress of bacterial FtsZ inhibitors with a focus on peptides. *FEBS J*. 2021;288(4):1091–1106. https://doi.org/10.1111/febs.15489

99 Gurnani M, Chauhan A, Ranjan A, et al. Filamentous thermosensitive mutant Z: an appealing target for emerging pathogens and a trek on its natural inhibitors. *Biology (Basel)*. 2022;11(5):624. https://doi.org/10.3390/biology11050624

100 Barrows JM, Goley ED. FtsZ dynamics in bacterial division: what, how, and why? *Curr Opin Cell Biol*. 2021;68:163–172. https://doi.org/10.1016/j.ceb.2020.10.013

101 Hong WL, Deng WY, Xie JP. The Structure, function, and regulation of mycobacterium FtsZ. *Cell Biochem Biophys*. 2013;65(2):97–105. https://doi.org/10.1007/s12013-012-9415-5

102 Lowe J, Amos LA. Crystal structure of the bacterial cell-division protein FtsZ. *Nature*. 1998;391(6663):203–206. https://doi.org/10.1038/34472

103 Nogales E, Wolf SG, Downing KH. Structure of the alpha beta tubulin dimer by electron crystallography. *Nature*. 1998;391(6663):199–203. https://doi.org/10.1038/34465

104 Fujita J, Maeda Y, Mizohata E, et al. Structural flexibility of an inhibitor overcomes drug resistance mutations in *Staphylococcus aureus* FtsZ. *ACS Chem Biol*. 2017;12(7):1947–1955. https://doi.org/10.1021/acschembio.7b00323

105 Alnami A, Norton RS, Pena HP, Haider S, Kozielski F. Conformational flexibility of a highly conserved helix controls cryptic pocket formation in FtsZ. *J Mol Biol*. 2021;433(15):167061. https://doi.org/10.1016/j.jmb.2021.167061

106 Musrati RA, Kollárová M, Mernik N, Mikulásová D. Malate dehydrogenase: distribution, function and properties. *Gen Physiol Biophys*. 1998;17(3):193–210.

107 Priestley JRC, Pace LM, Sen K, et al. Malate dehydrogenase 2 deficiency is an emerging cause of pediatric epileptic encephalopathy with a recognizable biochemical signature. *Mol Genet Metab Rep*. 2022;33:100931. https://doi.org/10.1016/j.ymgmr.2022.100931

108 Nian HJ, Li S, Wang J, et al. Expression, purification and functional characterization of two recombinant malate dehydrogenases from Mortierella isabellina. *Appl Biochem Microbiol*. 2019;55(3):224–230. https://doi.org/10.1134/S0003683819030098

109 Pradhan A, Tripathi AK, Desai PV, et al. Structure and function of *Plasmodium falciparum* malate dehydrogenase: role of critical amino acids in co-substrate binding pocket. *Biochimie* 2009;91(11–12):1509–1517. https://doi.org/10.1016/j.biochi.2009.09.005

110 Liu Q, Harvey CT, Geng H, et al. Malate dehydrogenase 2 confers docetaxel resistance via regulations of JNK signaling and oxidative metabolism. *Prostate* 2013;73(10):1028–1037. https://doi.org/10.1002/pros.22650

111 Romero AR, Lunev S, Popowicz GM, et al. A fragment-based approach identifies an allosteric pocket that impacts malate dehydrogenase activity. *Commun Biol*. 2021;4(1):949.

112 Botros N, Bell E, Bell J. The existence of a cryptic allosteric site on *Plasmodium falciparum* malate dehydrogenase. *FASEB J*. 2020;34:1–1. https://doi.org/10.1096/fasebj.2020.34.s1.05326

113 Botros N, Bell E, Bell J. Potential drug design for *Plasmodium falciparum* malate dehydrogenase targeting the cryptic allosteric site. *FASEB J*. 2021;35, https://doi.org/10.1096/fasebj.2021.35.S1.02936

114 He Y, Lei J, Pan X, Huang X, Zhao Y. The hydrolytic water molecule of Class A β-lactamase relies on the acyl-enzyme intermediate ES* for proper coordination and catalysis. *Sci Rep*. 2020;10(1):10205. https://doi.org/10.1038/s41598-020-66431-w

115 Bush K, Jacoby GA. Updated functional classification of beta-lactamases. *Antimicrob Agents Chempther*. 2010;54(3):969–976. https://doi.org/10.1128/AAC.01009-09

116 Alfei S, Schito AM. β-Lactam antibiotics and β-Lactamase enzymes inhibitors, Part 2: our limited resources. *Pharmaceuticals (Basel)*. 2022;15(4):476. https://doi.org/10.3390/ph15040476

117 Bush K. Past and present perspectives on beta-lactamases. *Antimicrob Agents Chemother*. 2018;62(10):e01076-18. https://doi.org/10.1128/AAC.01076-18

118 Chen J, Shang X, Hu F, et al. Beta-lactamase inhibitors: an update. *Mini Rev Med Chem*. 2013;13(13):1846–1861. https://doi.org/10.2174/13895575113139990074

119 Bonomo RA. beta-Lactamases: a focus on current challenges. *Cold Spring Harb Perspect Med*. 2017;7(1):a025239. https://doi.org/10.1101/cshperspect.a025239

120 Drawz SM, Bonomo RA. Three decades of beta-Lactamase inhibitors. *Clin Microbiol Rev*. 2010;23(1):160–160. https://doi.org/10.1128/CMR.00037-09

121 Sharma R, Park TE, Moy S. Ceftazidime-Avibactam: a novel cephalosporin/beta-lactamase inhibitor combination for the treatment of resistant gram-negative organisms. *Clin Ther*. 2016;38(3):431–444. https://doi.org/10.1016/j.clinthera.2016.01.018

122 Novelli A, Del Giacomo P, Rossolini GM, Tumbarello M. Meropenem/vaborbactam: a next generation beta-lactam beta-lactamase inhibitor combination. *Expert Rev Anti Infect Ther*. 2020;18(7):643–655. https://doi.org/10.1080/14787210.2020.1756775

123 Mansour H, Ouweini AEL, Chahine EB, Karaoui LR. Imipenem/cilastatin/relebactam: a new carbapenem beta-lactamase inhibitor combination. *Am J Health Syst Pharm*. 2021;78(8):674–683. https://doi.org/10.1093/ajhp/zxab012

124 Docquier JD, Mangani S. An update on beta-lactamase inhibitor discovery and development. *Drug Resist Updat*. 2018;36:13–29. https://doi.org/10.1016/j.drup.2017.11.002

125 Al Khamis M, AlMusa Z, Hashhoush M, Alsaif N, Salam A, Atta M. Carbapenem-resistant enterobacteriaceae: a retrospective review of presentation, treatment, and clinical outcomes in a tertiary care referral hospital. *Cureus*. 2022;14(7):e27094. https://doi.org/10.7759/cureus.27094

126 Bowman GR, Bolin ER, Hart KM, Maguire BC, Marqusee S. Discovery of multiple hidden allosteric sites by combining Markov state models and experiments. *Proc Natl Acad Sci U S A*. 2015;112(9):2734–2739. https://doi.org/10.1073/pnas.1417811112

127 Knoverek CR, Mallimadugula UL, Singh S, et al. Opening of a cryptic pocket in beta-lactamase increases penicillinase activity. *Proc Natl Acad Sci U S A*. 2021;118(47):e2106473118. https://doi.org/10.1073/pnas.2106473118

128 Horn JR, Shoichet BK. Allosteric inhibition through core disruption. *J Mol Biol*. 2004;336(5):1283–1291. https://doi.org/10.1016/j.jmb.2003.12.068

129 Hart KM, Moeder KE, Ho CMW, Zimmerman MI, Frederick TE, Bowman GR. Designing small molecules to target cryptic pockets yields both positive and negative allosteric modulators. *PLoS One*. 2017;12(6):e0178678. https://doi.org/10.1371/journal.pone.0178678

130 Avci FG, Altinisik FE, Karacan I, et al. Targeting a hidden site on class A betalactamases. *J Mol Graph Model*. 2018;84:125–133. https://doi.org/10.1016/j.jmgm.2018.06.007

131 Mikhnevich TA, Vyatkina Turkova AV, Grigorenko VG, et al. Inhibition of class A beta-Lactamase (TEM-1) by narrow fractions of humic substances. *ACS Omega*. 2021;6(37):23873–23883. https://doi.org/10.1021/acsomega.1c02841

132 Adams LA, Sharma P, Mohanty B, et al. Application of fragment-based screening to the design of inhibitors of Escherichia coli DsbA. *Angew Chem Int Ed*. 2015;54(7):2179–2184. https://doi.org/10.1002/anie.201410341

133 Sutoh S, Uemura Y, Yamaguchi Y, et al. Redoxtuning of oxidizing disulfide oxidoreductase generates a potent disulfide isomerase. *Biochim Biophys Acta Proteins Proteom*. 2019;1867(3):194–201. https://doi.org/10.1016/j.bbapap.2018.12.005

134 Martin JL, Bardwell JC, Kuriyan J. Crystal structure of the DsbA protein required for disulphide bond formation in vivo. *Nature*. 1993;365(6445):464–468. https://doi.org/10.1038/365464a0
135 Santos-Martin C, Wang GQ, Subedi P, et al. Structural bioinformatic analysis of DsbA proteins and their pathogenicity associated substrates. *Comput Struct Biotechnol J*. 2021;19:4725–4737. https://doi.org/10.1016/j.csbj.2021.08.018
136 Grauschopf U, Winther JR, Korber P, Zander T, Dallinger P, Bardwell JCA. Why is DsbA such an oxidizing disulfide catalyst? *Cell* 1995;83(6):947–955. https://doi.org/10.1016/0092-8674(95)90210-4
137 Guddat LW, Bardwell JC, Martin JL. Crystal structures of reduced and oxidized DsbA: investigation of domain motion and thiolate stabilization. *Structure* 1998;6(6):757–767. https://doi.org/10.1016/S0969-2126(98)00077-X
138 Charbonnier JB, Belin P, Moutiez M, Stura EA, Quemeneur E. On the role of the cis-proline residue in the active site of DsbA. *Protein Sci*. 1999;8(1):96–105. https://doi.org/10.1110/ps.8.1.96
139 Ren G, Stephan D, Xu Z, et al. Properties of the thioredoxin fold superfamily are modulated by a single amino acid residue. *J Biol Chem*. 2009;284(15):10150–10159. https://doi.org/10.1074/jbc.M809509200
140 Paxman JJ, Borg NA, Horne J, et al. The structure of the bacterial oxidoreductase enzyme DsbA in complex with a peptide reveals a basis for substrate specificity in the catalytic cycle of DsbA enzymes. *J Biol Chem*. 2009;284(26):17835–17845. https://doi.org/10.1074/jbc.M109.011502
141 Clatworthy AE, Pierson E, Hung DT. Targeting virulence: a new paradigm for antimicrobial therapy. *Nat Chem Biol*. 2007;3(9):541–548. https://doi.org/10.1038/nchembio.2007.24
142 McMahon RM, Premkumar L, Martin JL. Four structural subclasses of the antivirulence drug target disulfide oxidoreductase DsbA provide a platform for design of subclass-specific inhibitors. *Biochim Biophys Acta*. 2014;1844(8):1391–1401. https://doi.org/10.1016/j.bbapap.2014.01.013
143 Duprez W, Lakshmanane P, Halili M, et al. Peptide inhibitors of the Escherichia coli DsbA oxidative machinery essential for bacterial virulence. *J Med Chem*. 2014;58:577–587. https://doi.org/10.1021/jm500955s
144 Mou M, Yang W, Huang G, et al. The discovery of cryptic pockets increases the druggability of "Undruggable" proteins. *Med Res Rev*. 2025;45(6):1818–1849. https://doi.org/10.1002/med.70001